REPORT DOCUMENTATION PAGE

Form Approved
OMB No. 0704-0188

The public reporting burden for this collection of information is estimated to average 1 hour per response, including the time for reviewing instructions, searching existing data sources, gathering and maintaining the data needed, and completing and reviewing the collection of information. Send comments regarding this burden estimate or any other aspect of this collection of information, including suggestions for reducing the burden, to Department of Defense, Washington Headquarters Services, Directorate for Information Operations and Reports (0704-0188), 1215 Jefferson Davis Highway, Suite 1204, Arlington, VA 22202-4302. Respondents should be aware that notwithstanding any other provision of law, no person shall be subject to any penalty for failing to comply with a collection of information if it does not display a currently valid OMB control number.
PLEASE DO NOT RETURN YOUR FORM TO THE ABOVE ADDRESS.

1. REPORT DATE (DD-MM-YYYY)	2. REPORT TYPE	3. DATES COVERED (From - To)
March 31, 2005	Quarterly Report	1 Jan. to 31 Mar. 2005

4. TITLE AND SUBTITLE

Advanced Wireless Integrated Navy Network (AWINN)

5a. CONTRACT NUMBER

N00014-05-1-0179

5b. GRANT NUMBER

N00014-05-1-0179

5c. PROGRAM ELEMENT NUMBER

6. AUTHOR(S)

Warren Stutzman and Rick Habayeb

5d. PROJECT NUMBER

5e. TASK NUMBER

5f. WORK UNIT NUMBER

7. PERFORMING ORGANIZATION NAME(S) AND ADDRESS(ES)

Virginia Polytechnic Institute and State University
Electrical and Computer Engineering Department
302 Whittemore Hall (0111)
Blacksburg, VA 24061

8. PERFORMING ORGANIZATION REPORT NUMBER

1

9. SPONSORING/MONITORING AGENCY NAME(S) AND ADDRESS(ES)

Office of Naval Research
Ballston Centre Tower One
800 North Quincy Street
Arlington, VA 22217-5660

10. SPONSOR/MONITOR'S ACRONYM(S)

11. SPONSOR/MONITOR'S REPORT NUMBER(S)

12. DISTRIBUTION/AVAILABILITY STATEMENT

Approved for public release; distribution unlimited.

13. SUPPLEMENTARY NOTES

The views, opinions and/or findings contained in this report are those of the author(s) and should not be constructed as an official Department of the Navy position, policy or decision, unless so designated by other documentation.

14. ABSTRACT

Quarterly progress report No. 1 on AWINN hardware and software configurations of smart, wideband, multi-function antennas, secure configurable platform, close-in command and control for Sea Basing visualization of wireless technologies, Ad Hoc networks, network protocols, real-time resource allocation, Ultra Wideband (UWB) communications network and ranging sensors, cross layer optimization and network interoperability.

15. SUBJECT TERMS

16. SECURITY CLASSIFICATION OF:			17. LIMITATION OF ABSTRACT	18. NUMBER OF PAGES	19a. NAME OF RESPONSIBLE PERSON
a. REPORT	b. ABSTRACT	c. THIS PAGE			Rick Habayeb
U	U	U	UL		19b. TELEPHONE NUMBER (Include area code) 540-231-4353

Standard Form 298 (Rev. 8/98)
Prescribed by ANSI Std. Z39.18

Advanced Wireless Integrated Navy Network

AWINN

Quarterly Report 1

January 1, 2005 - March 31, 2005

Submitted to: Office of Naval Research

Attention: Santanu Das, Code 313

Submitted by: Virginia Tech

Attention: Warren Stutzman

ECE Dept.-0111

TABLE OF CONTENTS

Executive Summary

This first quarterly report presents the organization, plans, and schedule for the research effort in the following thrust areas:

Advanced Wireless Technology

Secure and Robust Networks

Visualization of Wireless Technology and Ad Hoc Networks,

Technology Integration Projects

In addition, the report provides details of initial progress and accomplishments in each task area.

The antenna group is concentrating on antennas for handheld devices, UWB, and the integration of antennas MIMO into the SDR and communications links. The Software Defined Radio group is investigating UWB software radios and the tradeoffs between range and data rate. They are evaluating various modulation schemes, including: OOK, PPM, PAM, and collaborative algorithm for distributed MIMO. The collaborative secure wireless communications team is investigating inter-sensor links of multi-node networks. The networking group is evaluating the metrics of mobile ad hoc networks, including: QoS, security, routing, and cross-layer optimization. The real-time system team is investigating time-utility function and distributed real time specification for Java to optimize resource allocation. The video communications group is investigating video in ad hoc networks and protocols for distributed sensors. The visualization of wireless technology team is focused on leveraging AWINN technologies to solve some of the operationally vexing problems of close-in Sea Basing challenges such as ranging for soft pickup and landing of cargo, ranging and imaging of ships during close-in maneuvers, and applying mesh MANET for distributed sensors.

Also during this reporting period, the AWINN team presented a comprehensive briefing on the program at the kickoff meeting on March 31, 2005, at Virginia Tech. The objectives and approaches of each project and task were presented.

1. TASK 1 Advanced Wireless Technologies

1.1 Task 1.1 Advanced Antennas

1.1.1 Overview

Task Goal: This task develops antennas for use in handheld and mobile terminals that require compact size and robust performance for both fixed and portable systems. The concepts will be extended to include fixed and portable terminal needs with emphasis on smart antennas, wideband antennas, MIMO and UWB antennas in support of the AWINN demonstrations.
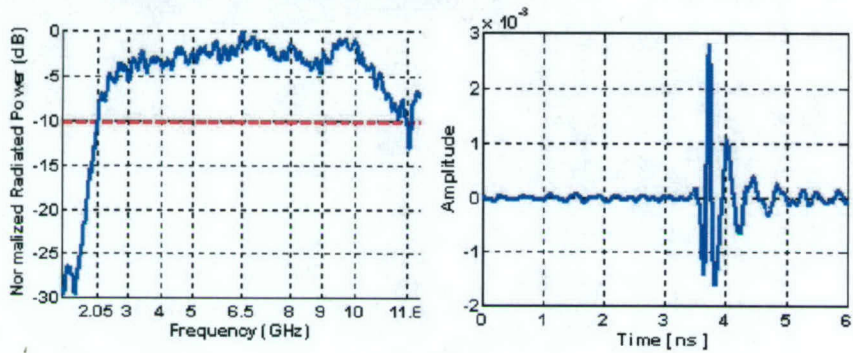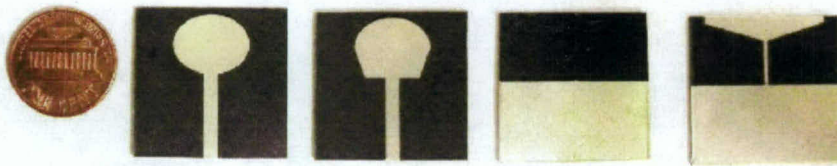
Directive terminal antennas allow improved anti-jamming effectiveness by limiting the radiation pattern with directional elements, possibly in a partitioned array. Base station antennas should emphasize the need for diversity. These antennas can be arrayed to provide polarization, spatial, and pattern diversity alternatives. Such antenna arrangements are also useful for MIMO and space-time coding processing systems to improve diversity and throughput. These subtasks support the demonstration of Task 4.

A new effort in UWB antennas will include the characterization of antennas for use in transient or wideband simulation and design. The characterization provides a minimal parameter description of the antenna properties. UWB offers a large potential for channel modeling as well as multipath mitigation over short distances. Support will also be given to Task 3 as the need requires in developing a physics/engineering-based template for radar simulation in an operational setting, including common EW techniques such as angle and range walk-off. Lastly, some effort will be devoted to the development of appropriate feed networks for wideband balanced antenna systems developed under the previous NAVCIITI program.
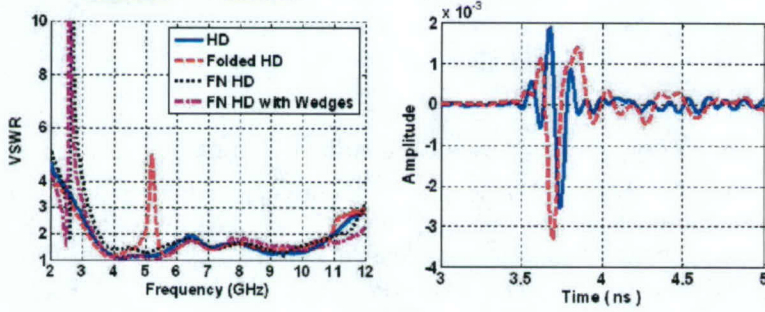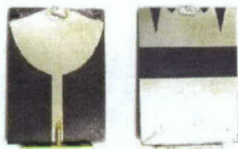
Organization: This task is managed by the Director of Virginia Tech Antenna Group (VTAG) using the following personnel:
    Bill Davis, task director
    Warren Stutzman, faculty
    Randall Nealy, engineer
    Taeyoung Yang, GRA

Summary: Effort of this first quarter was directed towards design and characterization of small UWB antennas for handheld and mobile terminals. The designed compact UWB antenna (Fig. 1.1-1a) covering 2.4 – 10.6 GHz has a penny size and narrow pulse width of less than 500 picoseconds. The frequency notch UWB antenna (Fig. 1.1-1b) successfully demonstrates the ability to place a rejection band within the operating band. A feasibility study was performed on the implementation of wearable UWB antennas based on UWB antenna design and characterization of the bulk camouflage fabrics (Fig. 1.1-1c). The pole-residue structure of the half-disk UWB antenna was also investigated (Fig. 1.1-1d). Five conference papers are to be published based on the results of the past quarter.

(a)

(b)

(c)

3

Impulse Response [ϕ = 00]

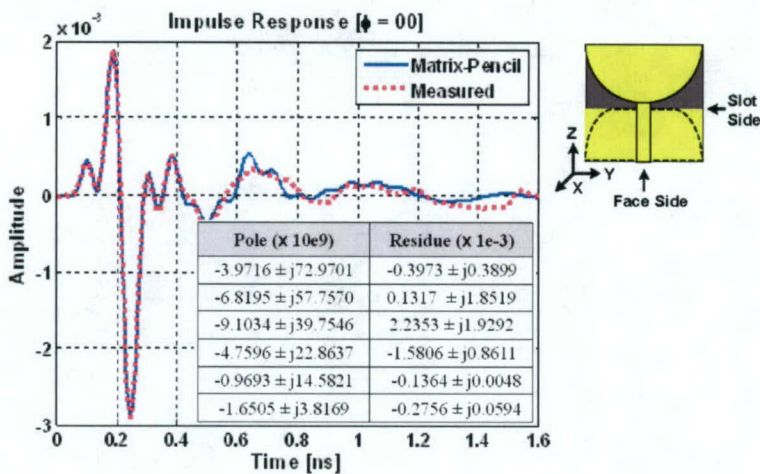| Pole (x 10e9)	Residue (x 1e-3)
-3.9716 ± j72.9701	-0.3973 ± j0.3899
-6.8195 ± j57.7570	0.1317 ± j1.8519
-9.1034 ± j39.7546	2.2353 ± j1.9292
-4.7596 ± j22.8637	-1.5806 ± j0.8611
-0.9693 ± j14.5821	-0.1364 ± j0.0048
-1.6505 ± j3.8169	-0.2756 ± j0.0594
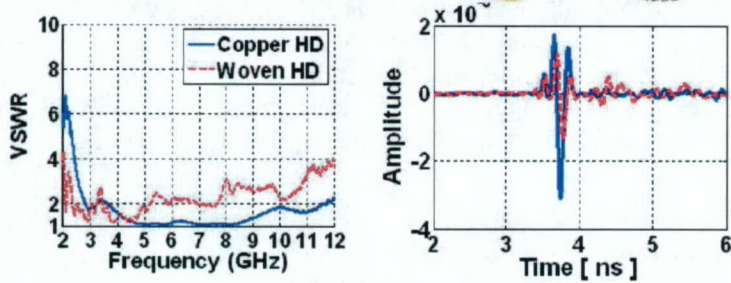
(d)

Figure 1.1-1 Antennas and associated measured data investigated this quarter. (a) Compact planar UWB antennas for mobile application (Subtasks 1.1a & b), (b) UWB antenna with frequency notch (Subtasks 1.1a & b), (c) Wearable UWB antenna (Subtasks 1.1a & b), and (d) Pole-residue model of half-disk UWB antenna with tapered ground (Subtask 1.1e).

1.1.2 Task Activities for the Period

Subtask 1.1a Investigation of compact antennas for handheld and mobile terminals

Task objective: Design compact planar UWB antennas for various applications and systems. Accomplishments during reporting period:

1. A new top-loaded ultra-wideband antenna covering both a 2.4 – 10.6 GHz impedance bandwidth (VSWR < 2.5) and the 2.05 – 11.6 GHz UWB band with nearly constant radiated power was designed and fabricated. The proposed antenna is a good candidate for backward compatibility of 802.11g in the 2.4 GHz ISM band, as well as providing an indoor/outdoor ultra-wideband frequency range of 3.1 – 10.6 GHz. In addition, it can be used for both multi-band OFDM and impulse UWB applications.

2. The new folded-notch half-disk antenna supports the dual bands of 2.4-2.5 and 3.1-10.6 GHz without increasing the size of the original UWB half-disk antenna covering only the UWB band. A parametric study demonstrated the effectiveness of controlling the location of the frequency notch and width of the additional operating band. The measured radiated power showed approximately 10 dB suppression at 2.6 GHz. The antenna has good impedance matching over both bands and an omni-directional radiation pattern. The link response showed a linear phase response versus frequency and narrow, transient pulse width. This antenna structure is a good candidate to support both 802.11g wireless LAN and indoor/outdoor UWB mobile applications.

3. Solid copper and woven versions of wearable half-disk antennas designed to cover 3.1–10.6 GHz showed good measured return loss characteristics, omni-directional patterns, and acceptable transient response. The results showed the wearable half-disk is a good candidate

for both multi-band OFDM and impulse UWB applications. However further study is required to improve the efficiency of the woven version.

4. Five conference papers were accepted; see Section 1.1.4

Links to other tasks: This task supports Tasks 1.2 and 4
Schedule: This task continues through the first year.
Personnel: Taeyoung Yang, GRA

Subtask 1.1b Antenna Characterization – transient & wideband
Task objective: Provide antenna characterization methods in both frequency and time domain
Accomplishments during reporting period:
1. Characterization of the designed compact planar UWB antennas with top-loading and frequency notch were performed in both frequency (radiation patterns, EIRP, and return loss) and time domain (link impulse response).

2. The relative permittivity and loss tangent for the camouflage cloth were estimated using microwave measurements with a TRL calibration and the two-microstrip-line method. The results showed that camouflage cloth has $\varepsilon_r \sim 1.5$ and *tan δ* ~ 0.02. The characterized information was used for the wearable UWB antenna design.

Links to other tasks: This task supports Task 1.1a, b, c, and e.
Schedule: This task continues through the first year.
Personnel: Taeyoung Yang, GRA

Subtask 1.1c UWB antenna design (support of AWINN demonstrations)
Task objective: Design various UWB antennas needed for AWINN demonstrations
Accomplishments during reporting period:
1. Reviewed the tentative specifications for the required UWB antennas.

2. Examined the feasibility of the given tentative specifications for the actual design.

3. Background literature review for the fundamental limit theory was conducted.

4. Using matrix pencil method, the pole-residue model of half-disk antenna was extracted from the measured transient data.

5. Two conference papers accepted on the following topics:

   – Fundamental Limits on Antenna Size and Performance.
   – The Planar UWB Antenna Response and UWB performance issues.

Links to other tasks: This task supports Tasks 1.2 and 4
Schedule: Initial design and fabrication will be done in the next 6 months and the performance improvement and optimization continues up to end of the year.
Personnel: Taeyoung Yang, GRA

Subtask 1.1d Antennas providing polarization, spatial, and pattern diversity – Evaluation of antennas in a MIMO environment
   This task has not started.

Subtask 1.1e Support physics/engineering-based models for Digital Ships

This task has not started.

Subtask 1.1f Wideband balanced antenna/array feed networks

This task has not started.

1.1.3 Importance/Relevance

- The designed compact planar UWB antennas can well accommodate the current needs for the handheld and mobile terminals.
- The designed frequency notch UWB antennas might provide a solution to reduce the inference to the existing other narrow band applications.
- The pole-residue model of the half-disk antenna supports complete mathematical description of the antenna characteristics. The model might be used for the communication link simulation including the antenna effects.

1.1.4 Productivity

Conference papers accepted for presentation:

1. Taeyoung Yang, William A. Davis, and Warren L. Stutzman, "Folded-Notch Dual Band Ultra-Wideband Antennas," IEEE AP-S International Symposium (Washington, DC), July 3-8, 2005.

2. Taeyoung Yang, William A. Davis, and Warren L. Stutzman, "Small, Planar, Ultra-Wideband Antennas with Top-Loading," IEEE AP-S International Symposium (Washington, DC), July 3-8, 2005.

3. Taeyoung Yang, William A. Davis, and Warren L. Stutzman, "Wearable Ultra-Wideband Half-Disk Antennas," IEEE AP-S International Symposium (Washington, DC), July 3-8, 2005.

4. Warren L. Stutzman, William A. Davis, and Taeyoung Yang, "Fundamental Limits on Antenna Size and Performance," Antenna Systems Conference (Santa Clara, CA), Sep. 22-23, 2005

5. Taeyoung Yang and William A. Davis, "The Planar UWB Antenna Response and UWB performance issues," General Assembly of International Union of Radio Science (New Delhi, India), Oct. 23-29, 2005.

Students supported

Taeyoung Yang, Jan. 15, 2005 – present

Faculty supported

Dr. William A. Davis, VTAG Director, Jan. 15, 2005 – present

Staff and other personnel supported

Mr. Randall Nealy, VTAG Engineer, Jan. 15, 2005 - present

1.2 Task 1.2 Advanced Software Defined Radio

1.2.1 Overview

Task Goal: This task investigates an advanced Software Defined Radio (SDR) which can take advantage of the unique properties of Ultra Wideband communication for Navy applications, such as precision position location, ranging, and low probability of intercept.

Organization: This task is managed by the Deputy Director of the Mobile and Portable Radio Research Group (MPRG) using the following personnel:

Jeffrey H. Reed, task director
R. Michael Buehrer, faculty
William H. Tranter, faculty
Chris R. Anderson, GRA
Swaroop Venkatesh, GRA
Jihad Ibrahim, GRA
Maruf Mohammad, GRA

Summary: This quarter we focused on developing a prototype version of the SDR receiver. A system simulation for the UWB version of the SDR receiver has been performed for both an AWGN and a simple 3-path multipath environment. These simulation results indicate that the performance of the SDR should be within a few dB of the theoretical maximum. Additionally, several design features, such as a data capture mode, have been incorporated into the receiver design to support the other AWINN activities.

SDR algorithm development during the past quarter focused on increasing the performance of signal acquisition, as well as data demodulation for UWB transmissions. UWB propagation environments are very rich in resolvable multipath, which makes a simple correlator matched to the transmit pulse shape highly inefficient. Research has mainly concentrated on Rake receivers as candidates for efficient UWB detectors, because of the inherent fine time resolution of the UWB pulse. We are investigating the use of pilot-based data demodulation, where pilot symbols are generated from both dedicated pilot pulses as well as data pulses. Incorporating both pilot and data pulses into the matched filter template waveform reduces training overhead and can improve system performance.

Recent developments in light-weight multi-mode/multi-band software radios can leverage a multi-band communication capability and network-wide position location information to achieve the same benefits offered by space-time coding (STC) and multiple-input-multiple-output (MIMO) communication systems without the use of antenna arrays. In particular, we are working on adapting such a distributed MIMO communication system to operate using UWB signals to improve the range and performance of UWB communication links.

For ranging and position location, initial algorithms have been developed and tested in a simple proof-of-concept laboratory environment. The results indicate that ranging accuracy should be within a few inches, and that position location via evaluation of the multipath delay profile is possible. These algorithms are currently being updated to provide full 3-D ranging and positioning information, as well as incorporate the use of the SDR receiver.

1.2.2 Task Activities for the Period

Subtask 1.2a Develop flexible software radio platforms that include cross-layer optimization with capabilities for UWB and ad hoc networking

Task objective: The overall goal of this subtask is to design an advanced software-defined/reconfigurable radio that is optimized for ultra wideband communication, and then to implement the system using off-the-shelf components.   The software-defined radio implementation provides tremendous flexibility compared to a single hardware implementation—for example, providing the capability to utilize one of several different popular UWB modulation or multiple access schemes, to operate in one of several modes (communication, ranging, or data capture), as well as to utilize more traditional broadband communication schemes. In order to leverage MPRG's existing experience in board- and system-level design the communication system will be implemented using commercially available off-the-shelf (COTS) components.

The advanced SDR receiver is based on a Time Interleaved Sampling (TI-Sampling) architecture with digital demodulation. The basic concept is to oversample the analog received signal (sample at equal to or greater than twice the Nyquist frequency) and then to perform demodulation in the digital domain using a Xilinx Virtex-II Pro FPGA. The idea behind TI-Sampling is to relax the requirements on the ADC-to-FPGA data bus while still maintaining a high sampling rate; this is a quite common technique for high-speed oscilloscope design. Essentially, the received waveform is sampled by a number of ADCs operating in parallel, with each ADC clock slightly offset from the others, as shown in Figure 1.2-1. Thus, each ADC samples a slightly different point of the time-domain waveform, and the effective sampling rate is the individual ADC sample rate multiplied by the total number of ADCs, as illustrated in Figure 1.2-2.

The primary design trade-off in a TI-Sampling receiver is complexity: instead of a single high-speed data bus, the receiver now has several lower-speed busses. Additionally, the use of multiple ADCs will increase the power consumption and PCB area required to implement the receiver. Finally, small imperfections in the clock signal delay, as well as clock jitter, and ADC aperture delay will lead to slight variations in the exact point at which each ADC samples—resulting in distortion of the received signal.
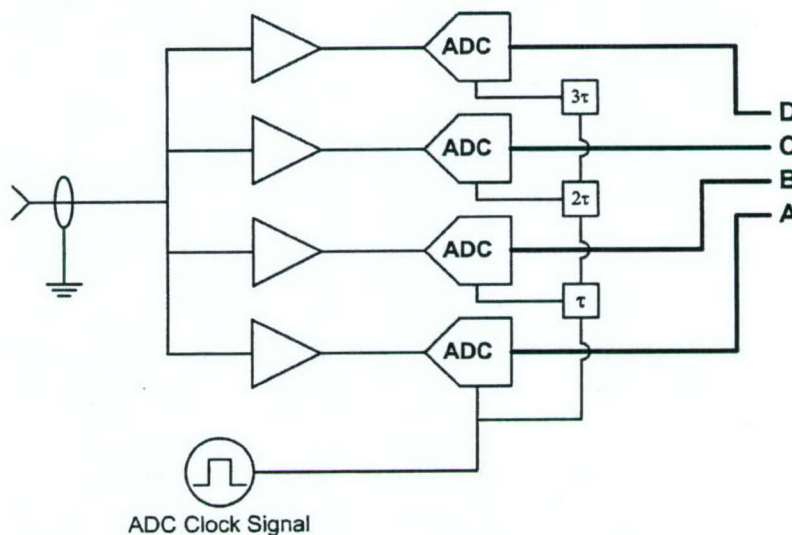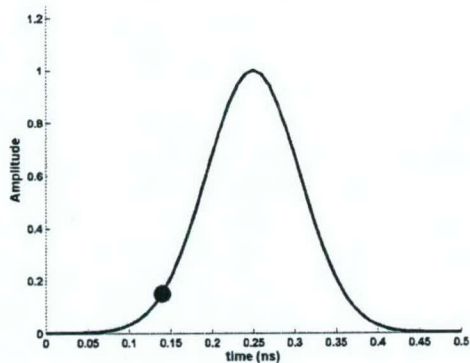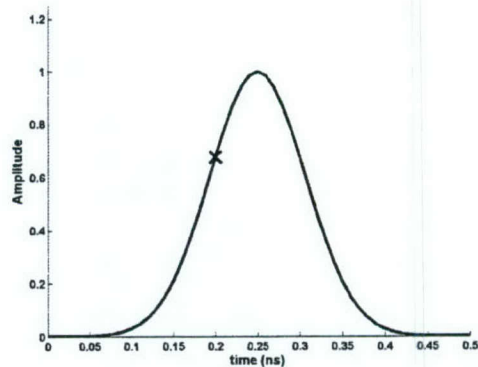

Figure 1.2-1 Block diagram of the TI sampling architecture for 4 ADCs.

For UWB communication, the receiver is configured to operate as a Digital Pilot-Based Matched Filter (DPBMF) receiver, which is functionally similar to the Matched Filtering receiver that has been used in narrowband communications for many years. At the beginning of every data frame, the transmitter sends a series of pilot pulses. The receiver then captures the ADC samples associated with the pilot pulses, stores them in the FPGA's memory, and then averages samples from successive pulses together to produce a single template waveform. Included in the template is any resolvable multipath, which improves the performance of the receiver in multipath environments without the need to implement complex RAKE algorithms. The stored template pulse is then correlated with the data pulses via a standard matched filtering operation.

The advantage of the DPBMF design is that it is able to track distortions/variations in the received pulse, so that even in non-line of sight scenarios, the averaged template should compensate for any pulse distortion in the received data pulses. The primary drawback to DPBMF is that the template will contain noise and other extraneous signals. The BER performance of the DPBMF receiver is therefore somewhat degraded compared to a receiver that uses an ideal template waveform. The cause of the degradation is a "noise-cross-noise" term, due to the multiplication of the noise in the template by the noise in the received signal. The impact of the noise term can be reduced by increasing the number of pilot symbols, but at the expense of a reduction in the data rate.
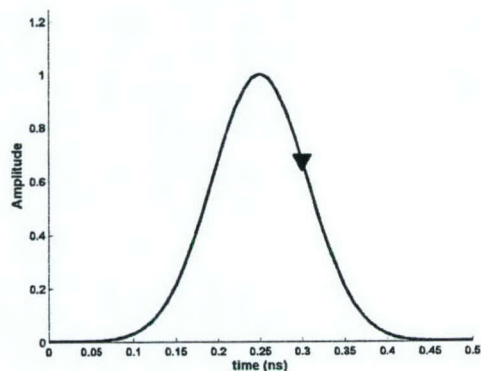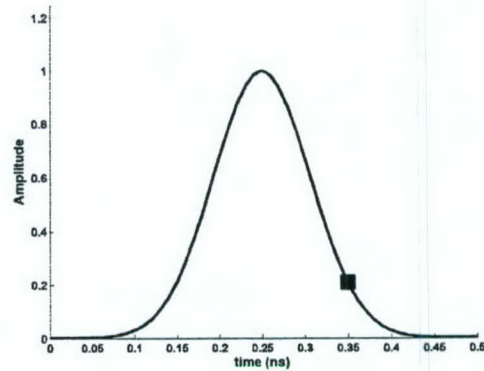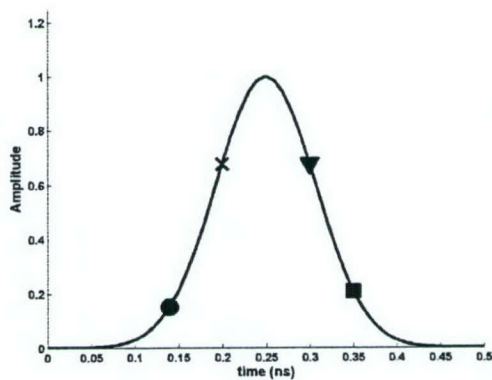
Figure 1.2-2 Graphical representation of the TI sampling Architecture. (a) ADC #1 samples the signal at Point A, (b) ADC #2 samples the signal at Point B—a time offset of τ relative to ADC #1, (c) ADC #3 samples the signal at Point C—a time difference of τ relative to ADC #2, (d) ADC #4 samples the signal at Point D—a time difference of τ relative to ADC #3, (e) The original waveform may be reconstructed by putting all 4 samples together.

Accomplishments during reporting period: The block diagram of the SDR receiver is shown in Figure 1.2-3. The receiver is composed of 4 major subsystems: the analog RF front end, the ADC and clock distribution bank, the FPGA, and a USB 2.0 interface device. The RF front end utilizes a number of ultra-broadband amplifiers, attenuators, and filters and feeds the received signal to the ADCs. A bank of 8 MAX104 ADCs, each sampling at a frequency of 1 GHz, are used to achieve an aggregate sampling frequency of 8 GHz. Sampled data are then input into a Xilinx XC2VP70 FPGA, which performs digital processing. The USB interface provides a high-speed communication link with a host computer.
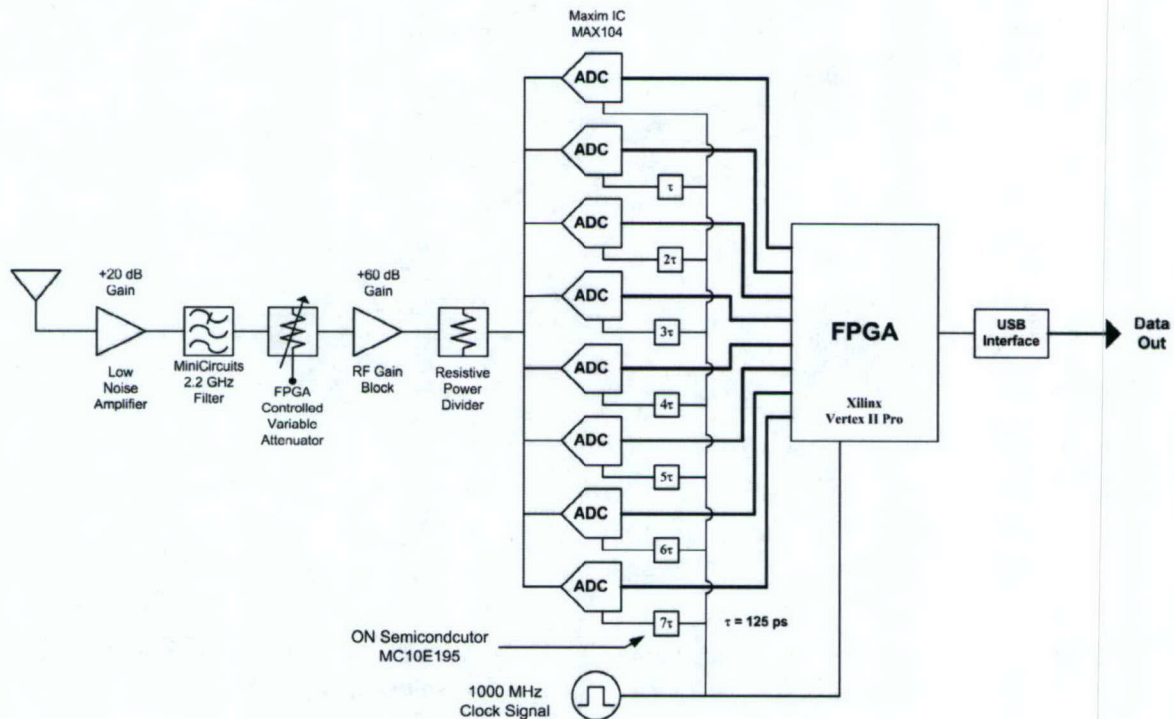

Figure 1.2-3 Block diagram of the advanced SD receiver.

A thorough system simulation has been performed to evaluate the performance of the receiver for Pulse Amplitude Modulation (PAM) and Pulse Position Modulation (PPM) in both AWGN and a simple three-path multipath environment. The multipath simulation was set up such that no intersymbol interference occurred (i.e. the maximum delay for a multipath signal was less than the time between transmissions of UWB pulses). The BER results for 2-PAM modulation are shown in Figure 1.2-4 along with the theoretical BER for a noiseless template waveform; the BER results for 2-PPM are shown in Figure 1.2-5 along with its theoretical curve. As expected, the results for the DPBMF receiver are slightly worse than a perfectly matched receiver due to the noisy nature of the pilot-based matched filter template used in data demodulation. In this simulation, 27 pilot pulses were averaged to form the data demodulation template, and the simulation assumed one UWB pulse was transmitted for every one data bit. The BER performance could be improved by including more pilot pulse in the template waveform or by transmitting multiple UWB pulses per data bit, but at the expense of data throughput.

11

Compared with the AWGN channel, the DPBMF receiver performs slightly worse in a multipath environment due to the decrease in the addition of noise in the template due to more energy per bit. One interesting result is that the performance degradation for 2-PPM in a multipath channel is greater than for 2-PAM. The reason is that information in PPM is contained in the precise timing of the pulse, making it significantly more sensitive to channel dispersion, because orthogonality is lost. The loss in orthogonality causes the probability of detecting a "1" to be greater than the probability of detecting a "0", leading to a higher BER.
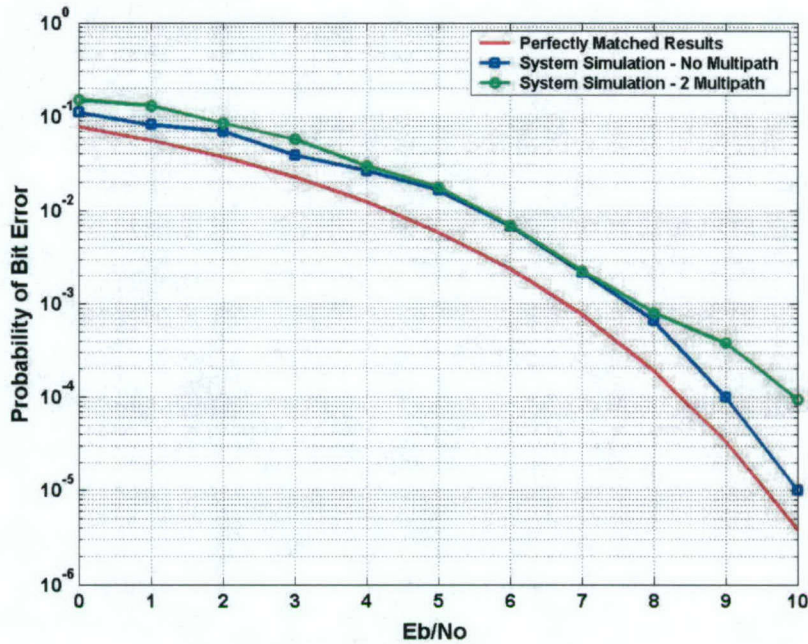
Figure 1.2-4 BER curves assuming perfect synchronization for 2-PAM in a 3-path multipath channel with no ISI and 2-PAM in an AWGN channel, both using 27 pilots.
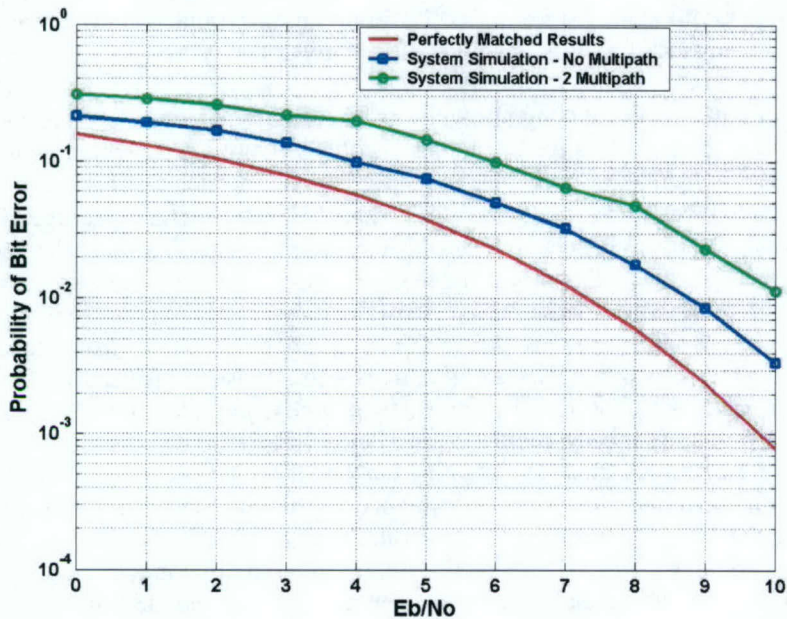
Figure 1.2-5 BER curves assuming perfect synchronization for 2-PPM in a 3-path multipath channel with no ISI and 2-PPM in an AWGN channel, both using 27 pilots.

Schedule:
- January – June 2005
  - Develop 2-ADC Prototype Receiver
- Summer 2005
  - Fabricate Receiver
    - Update Transmitter Design
    - Evaluate Prototype Receiver Hardware and FPGA Code
- Fall 2005
  - Develop 8-ADC Full Receiver
    - Begin Integration of Receiver with Other AWINN Activities
- 1st Quarter 2006
  - Fabricate Receiver
  - Verify Operation of Receiver Hardware and FPGA Code
- 2nd Quarter 2006
  - Demonstrate Transceiver Operation
  - Integrate Transceiver with Other AWINN Activities

Personnel:
  Chris R. Anderson – Transmitter and Receiver Hardware Development
  Deepak Agarwal – Receiver FPGA Code Development

Subtask 1.2b Software radio research applied to UWB, including design parameter space exploration.

Task objective: The objective of this task is to investigate innovative SDR architectures and algorithms for both traditional broadband and UWB communications. These algorithms will be implemented on the advanced SDR receiver developed in Subtask 1.2a.

Indoor UWB systems have to contend with extremely frequency-selective communication channels. The received signal is very rich in resolvable multipath, which makes a simple correlator matched to the transmit pulse shape highly inefficient. Research has mainly concentrated on Rake receivers as candidates for efficient UWB detectors, because of the inherent fine time resolution of the UWB pulse. However, it has been shown that the Rake energy capture is relatively low for a moderate number of fingers, making its implementation impractical for UWB systems. The pilot-assisted receiver is another widely studied type of receiver which aims at gathering all the signal energy by using the received pulse shape itself as a correlation template. Pilot-assisted receivers suffer from a "noise-cross-noise" term, caused by the use of a noisy signal as a correlation or matched filter template. Consequently, a prohibitively large number of pilots are required to overcome this limitation. The training overhead can be reduced by using a data-aided pilot-assisted scheme, where channel information is jointly extracted from the training and data signals. However, performance is still limited by the low SNR operating levels of traditional UWB systems. A potential solution is to add a strong error correcting code. Error correction coding is especially attractive for systems employing low-duty cycle pulses, since coding can be added while maintaining the data rate by reducing the symbol repetition time.

Accomplishments during reporting period:

Pilot-assisted, Data-aided UWB Receiver with FEC

We aim for a receiver where the entire received energy is captured while maintaining a "clean" template for a limited number of pilots. Since both pilot and data signals contain information about the channel, the training overhead can be reduced by incorporating both into an iterative template construction algorithm.

The receiver works as follows. First, an initial template $v_o(t)$ is generated using a training frame of Np pilot signals:

$$v_0(t) = \frac{1}{N_p}\sum_{j=1}^{N_p} r_{pj}(t), \text{ where } r_{pj}(t), \text{ is the } j^{th} \text{ pilot signal.}$$

Then, the data bits are estimated and used to construct an improved estimate. Assuming binary biphase modulation, and a data frame consisting of N_d signals $r_{di}(t)$, $1 \pounds i \pounds N_d$, and noting $\hat{b}_{in}$ as the estimated i^{th} bit at the nth iteration, the template at the nth iteration is defined by:

$$v_n(t) = \frac{1}{N_d}\sum_{i=1}^{N_d} \hat{b}_{in}\, r_{di}(t), n > 1$$

An improved template results in more bits being detected correctly, which in turn produces a cleaner template. Unlike the pure pilot-based receiver, a small number of pilots can be tolerated, because $v_0(t)$ is not the final template. However, for this scheme to operate efficiently, N_p must be large enough to provide a good starting point for the iterative process. The quality of the template is limited by the low instantaneous signal energy due to the dispersive channel. This can be

solved by adding a strong error correcting code. We use systematic LDPC codes, which are linear block codes based on a large, sparse parity check matrices. Decoding is based on the iterative belief propagation algorithm. The receiver uses an iterative decoding approach which takes advantage of the systematic bits in the decoded message to re-estimate the template. The potential efficiency of the proposed system (Figure 1.2-6) lies in the following synergy: in order to yield significant coding gain, the decoding scheme requires an adequate energy capture level, which is provided by the improved template. Moreover, the coding gains lead to more bits being decoded correctly, thus forming a cleaner template.
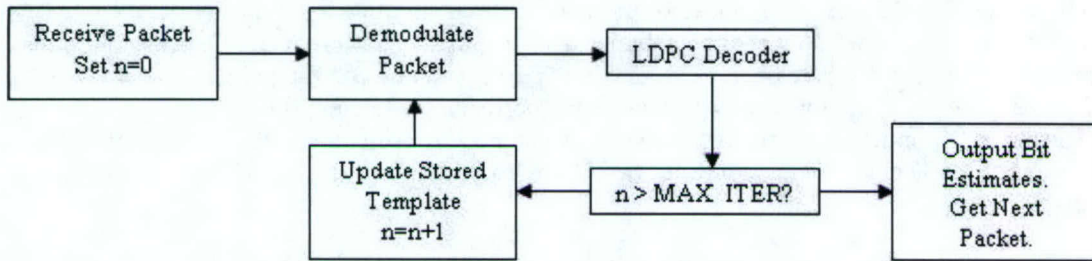
Figure 1.2-6 Pilot-based, data-aided, LDPC receiver.

The proposed system performance is illustrated in Figure 1.2-7. We employ indoor non-line of sight channel measurements taken at MPRG. A Gaussian monocycle of duration 500 psec is used. The proposed coded system employs a rate 1/2 systematic LDPC code, with N_d=541 and N_p=50, and 3 template iterations per data frame. First, notice a data-aided scheme outperforms the traditional pilot-based scheme. Secondly, the coded system without data-aided template fails, because the decoding fails due to the dirty template. The coded system with data-aided template estimate is vastly superior. This illustrates the synergy created between coding and template estimation in our iterative scheme.

Figure 1.2-7 Error rate performance of proposed system.

Acquisition

The design of fast and efficient synchronization, or acquisition, schemes is a challenging aspect of UWB. Traditional synchronization techniques used in spread spectrum (SS) systems are not suitable for UWB, mainly because they result in prohibitively long acquisition times. In fact, due to the use of extremely short, low duty cycle UWB pulses, the delay uncertainty region contains a huge number of potential timing offsets, or cells, compared to narrowband systems. Designing efficient search algorithms that efficiently proc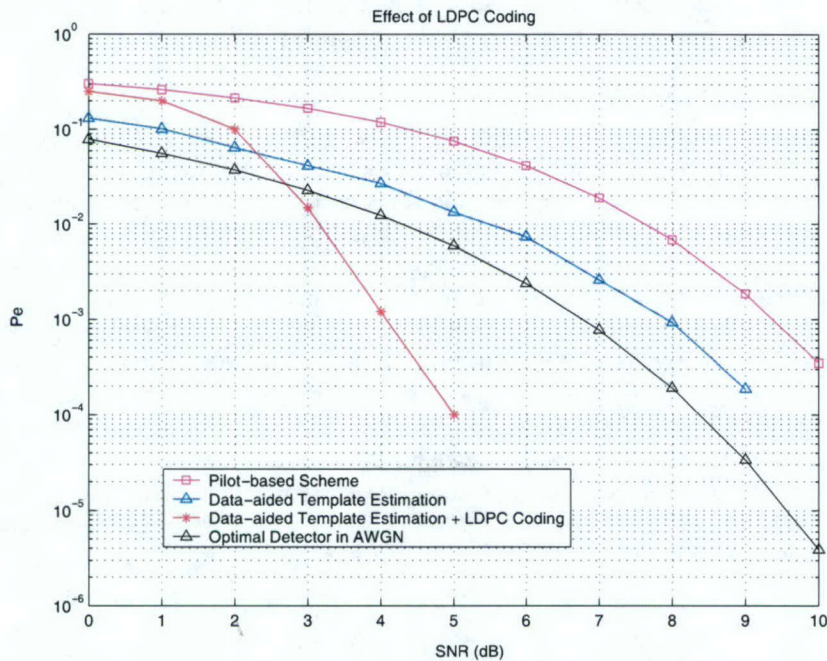ess those cells has been the main focus of research in UWB acquisition to date. In addition to the long acquisition time, the problem of UWB synchronization is further complicated in indoor dense multipath channels, where energy dispersion makes it hard to generate reliable decision metrics. Moreover, whereas traditional acquisition strategies for SS systems assume that there is a single correct cell (termed an H_1 cell) within the uncertainty region which represents the correct signal delay, this assumption does not hold for UWB in multipath, because of the large number of resolvable paths. Instead, there will be a group of H_1 cells corresponding to the different multipath delays which can terminate the acquisition process.

Most references assume that acquisition is successful if any H_1 cell is detected. However, this assumption is highly unsuitable for UWB applications operating in dense multipath. In fact, for UWB ranging applications, the detected multipath might be tens of nanoseconds away from the start of the signal due to the large delay spread, resulting in ranging errors in the tens of feet. This approach is also inefficient in communication applications, since locking to an arbitrary multipath and assuming it to be the earliest arriving path might lead to a loss of a large part of the symbol energy, resulting in substantially higher symbol error probabilities. The problem is not trivial, since the LOS path might not be the strongest path. Moreover, it might be severely attenuated, which makes its detection with high probability a challenging task.

The main challenge for UWB synchronization in dense multipath is therefore to design acquisition algorithms that are able to accurately detect the first arriving multipath, while minimizing the acquisition time. One such algorithm is presented here.

Two-Stage UWB Acquisition

A two-stage acquisition technique is proposed, where the first stage termed *coarse acquisition* simply finds any of the many multipath components (i.e., simply achieves rough symbol/code synchronization). The main requirement for this stage is that it must detect a multipath as fast as possible. In the proposed implementation, the first stage is a fast version of traditional threshold comparison serial test, called *jump-phase* search, where the search time is drastically reduced by performing a non-consecutive search, where the H_1 cells are uniformly spread over the uncertainty region. The procedure does not add any significant complexity to the circuit compared to serial search, and knowledge of the number of multipath components is not needed. Although this stage might not necessarily lock to the desired path, it allows the uncertainty region (in which the desired path exists) to be reduced considerably. The second stage, termed *fine acquisition*, searches for the first arriving path in the reduced uncertainty region. The second stage takes advantage of a robust estimate of the noise variance, obtained from the first stage, to calculate a new, more reliable threshold. Moreover, it exploits the clustered nature of the multipath to better segregate H_0 cells (cells corresponding to incorrect delays) from H_1 cells, and more reliably detect the start of the signal, even when the LOS path is severely attenuated.

Coarse Acquisition

Serial (or linear) search is the most popular acquisition technique for practical systems. In serial search, the cells in the uncertainty region are searched consecutively, in the order in which they

16

occur in time (Figure 1.2-8). Since no *a priori* timing information exists, it is assumed that the search start position is uniformly distributed over the uncertainty region, that is, the probability of starting the search at an arbitrary cell is equal to $1/C$, where C is the total number of cells.

The key to reducing the mean acquisition time in dense multipath is to search the multipath components in non-consecutive order. One such method is *bit reversal* search, where the binary representation of the cell indices are 'bit-reversed' and searched in a new order. This strategy maximizes the distance between consecutively tested cells, and is shown to yield similar performance to the prior search at high SNR. However, there is an inherent added complexity involved in performing the bit reversal and modifying the delay from one cell to another, especially for a large number of cells. Moreover, the procedure is further complicated when the number of cells is not a power of two, which is usually the case. We propose a simple search algorithm, named *jump-phase* search, which does not add any significant complexity compared to serial search, and does not assume knowledge of the number of multipath components. In the jump-phase search, the jump between cells is equal to C_{in}, where C_{in} is the number of cells in one particular spreading code phase duration T_f. Note that C_{in} is independent of the channel profile. By using this search, the H_I cells are uniformly spread over the uncertainty region (Figure 1.2-8). An H_I cell is visited every C_{in} cell. The search becomes more efficient as the number of resolvable multipath components increases, and more H_I cells terminate the search. Since UWB inherently possesses a fine time resolution, we expect the acquisition time to be reduced drastically compared to serial search.
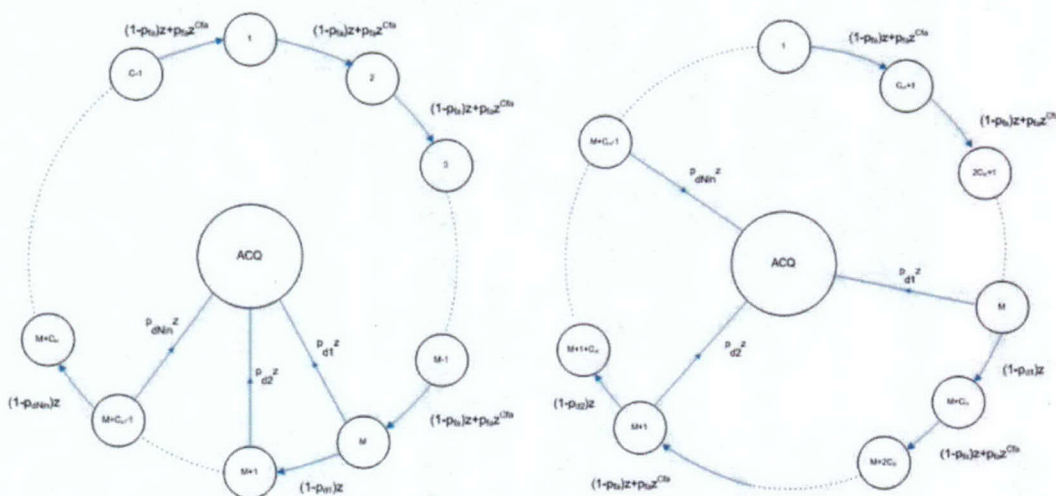
Figure 1.2-8 Serial search (left) versus jump search (right). In jump search, H_I cells are unifromly spread over uncertainty region.

Fine Acquisition
The coarse acquisition stage locks onto an arbitrary multipath component. This is unsuitable for both ranging and communications applications, since it respectively leads to large ranging errors and significant loss in symbol energy capture. We propose a method to capture the earliest arriving path in this section.
Let $\hat{\tau}$ be the delay estimated by the first stage. Since the H_I region spans T_f seconds, we know that the first arriving path delay belongs to the interval $[\hat{\tau} - T_f, \hat{\tau}]$. The fine acquisition stage performs an additional search in this reduced uncertainty region. This stage is formed the two steps described in the following.

First, a threshold crossing test is performed, using a newly calculated threshold. In the coarse acquisition stage, the noise power is unknown and the threshold setting mechanism cannot take SNR information into account with a simple procedure. However, since the H_l region has been identified to within C_{in} cells at the end of coarse acquisition, an estimate of the noise variance can now be obtained by calculating the average of the decision statistics over the H_0 region. Then, an additional test is performed to segregate H_0 cells and detect the earliest H_l cell, by taking advantage of the clustered nature of the multipath channel. The surviving cells form the first step are further processed as follows: For a particular surviving cell X_k, if the closest surviving cell X_{k+1} is more than s seconds away from X_k, X_k is eliminated. After all cells are tested, the earliest surviving cell is selected. The rationale behind this method is based on the clustered nature of multipath. Since multipath occurs in clusters, it is most likely that the multipath cluster will result in a group of neighboring surviving cells. If, on the other hand, an isolated cell exceeds the threshold, it is most likely an H_0 cell.

Results

Figure 1.2-9 illustrates the mean acquisition time (in number of cells visited) for serial, bit reversal and jump phase search, respectively. Note that jump-phase search results in significant reduction in acquisition time compared to serial search, and only slight degradation compared to bit reversal, at the expense of a simpler search mechanism.

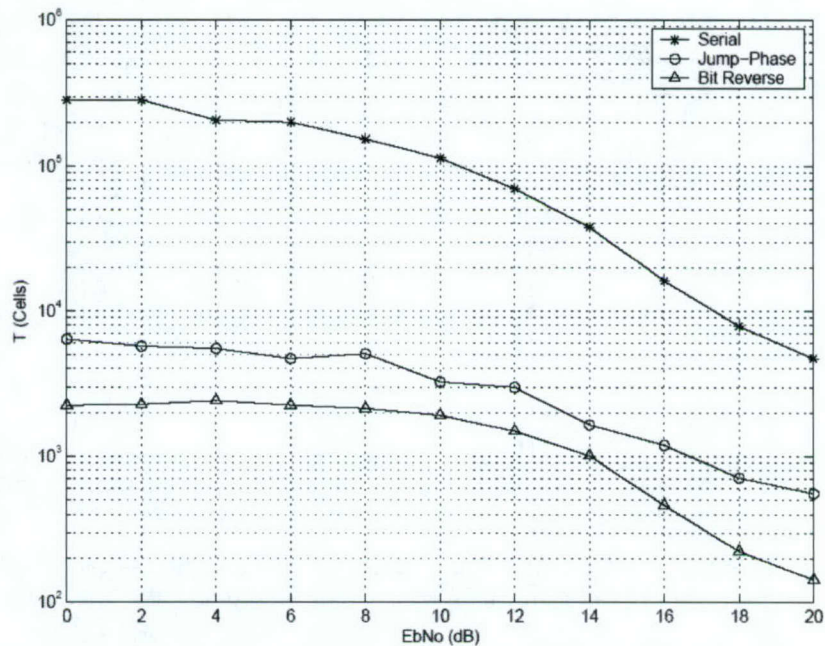**Figure 1.2-9** Mean acquisition time for bit reversal, jump phase, and serial search. Spreading code length = 32.

The application of fine acquisition to ranging is illustrated in Figure 1.2-10. The acquisition error τ is mapped into a ranging error d by $d = ct$, where c is the speed of light. Notice that fine acquisition results in significant reduction in ranging error compare to traditional acquisition (serial search).
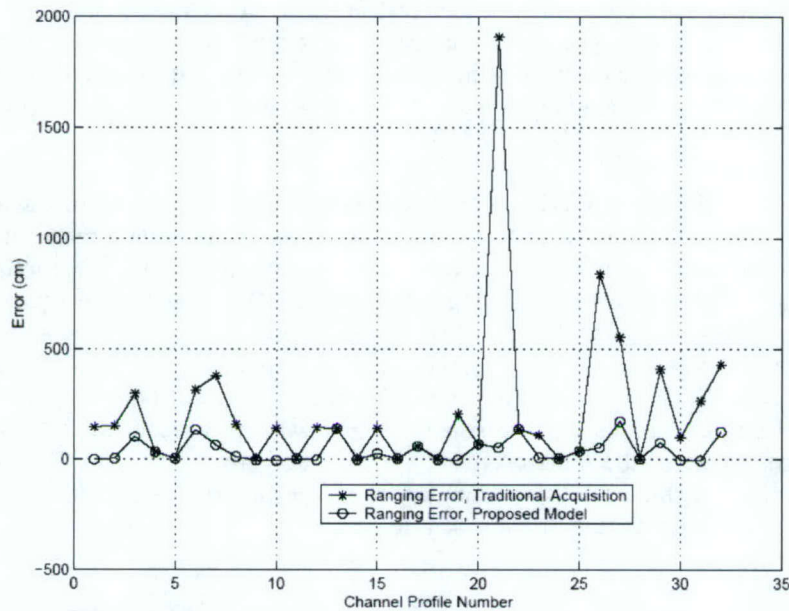
Figure 1.2-10 Performance of fine acquisition in ranging. SNR = 15 dB. Spreading code length = 64.

Schedule:
- January-Summer 2005
  - Finalize two-stage acquisition algorithm
  - Investigate further receiver design strategies
- Summer-Fall 2005
  - Start work on narrowband interference mitigation techniques
  - Start work on UWB tracking
  - Finalize receiver design algorithms
- 1st Quarter 2006
  - Finalize interference work
  - Begin integrating algorithms into hardware
- 2nd Quarter 2006
  - Integration of interference cancellation, synchronization and signal detection into common framework

Personnel:
Jihad Ibrahim – UWB Algorithm Development

Subtask 1.2c Software radio designs for collaborative systems that take advantage of this radio, particularly for interference environments.

Task objective: The cost, weight, and poor aero-dynamics of antenna arrays greatly limit their practical use on both unmanned vehicles and dismounted tactical warfighters. However, recent developments in light-weight multi-mode/multi-band software radios can leverage a multi-band communication capability and network-wide position location information to achieve the same benefits offered by space-time coding (STC) and multiple-input-multiple-output (MIMO) communication systems without the use of antenna arrays. In this case, communication nodes in a tight cluster can coordinate both their transmissions and receptions to mimic an STC's operation

19

as if they were part of a single antenna array platform. This novel technique, which we call *synthetic STC* (SSTC) can significantly extend the range of long-haul cluster-to-cluster communications. The objective of this research effort is to perform a design study and understand the benefits of SSTC for SDR radio networks in facilitating the Navy's 'toughest' communication needs.

Applying distributed MIMO to UWB communications provides a number of advantages over SISO UWB channels, including: higher spectral efficiency or faster data rates, improved link reliability through diversity gain, range extension through coordinated transmissions, and nodes can take advantage of the sensing and ranging properties of UWB signals. An example of such a network is shown below in Figure 1.2-11. This network consists of a large number of low-power UWB nodes, each of which has a fairly limited range. If one or more of the nodes needs to transmit data outside its range, it can form a collaborative "team" of nodes. The collaboration effectively forms a time-domain macro diversity system, which increases the transmitted power and effectively the range of the local network. The collaborative algorithms developed in this subtask will be verified through system simulation as well as implementation on a set of the advanced SDR receivers developed in Subtask 1.2a.
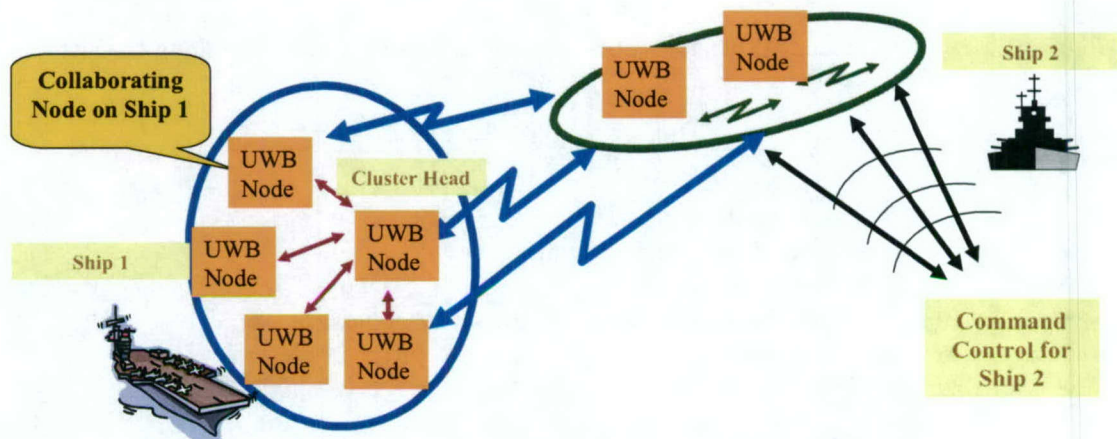

Figure 1.2-11 Illustration of distributed MIMO using UWB signals.

Schedule:
- January-Summer 2005
  - Develop UWB MIMO Algorithms
- Summer-Fall 2005
  - Simulate performance of UWB MIMO Algorithms
- Spring 2006
  - Begin Work on testing algorithms on Advanced SDR Receiver

Personnel:
Jeffrey H. Reed

Subtask 1.2d Vector channel models, including Markov Models, and supporting channel measurements.

Task objective: Hidden Markov Models (HMM) for wireless channels are convenient and analytically tractable tools that describe the statistical behavior of a complicated random time series. For example, HMM can be used to evaluate the behavior of a wireless signal in a fading channel. Cognitive radios could use HMM to track variations in the channel; these radios could then respond in a manner that mitigates the effects of these changes. The objective of this subtask is to develop algorithms to establish appropriate HMM model for a given application. These models and algorithms will then be verified via simulation and possibly by experimental data using the advanced SDR receiver.

Schedule:
–   January-Summer 2005
    •   Collect channel measurements
–   Summer-Fall 2005
    •   Begin model development
–   1st Quarter 2006
    •   Simulate performance of the models for UWB communications
–   2nd Quarter 2006
    •   Integrate models with SDR Receiver

Personnel:
    Maruf Mohammad – HMM Algorithm Development

Subtask 1.2e Software radio integration into the AWINN demonstrations.

Task objective: The goal of this subtask is to integrate the software radio developed in Subtask 1.2a into AWINN activities. To achieve this objective, the software radio is being designed with two distinct modes of operation: a communication mode and a data capture mode. The communication mode is currently optimized for impulse UWB signals, however, it is capable of operating using any broadband communication technique (such as DSSS or OFDM). The only limitations on the types of signals that the receiver can handle are: (1) the 2.2 GHz analog input bandwidth limitation of the MAX104 ADCs, (2) the 8 GHz effective receiver sampling frequency, and (3) the processing power of the FPGA.

In the data capture mode, the receiver will simply capture ADC samples and store them in the FPGAs RAM memory. The data can then be processed in non-real time using one of the FPGAs PowerPC processors, or the sample values can be transmitted to a host computer via the USB interface. The number of samples that can be captured is limited by the amount of high-speed RAM memory that can be allocated, but is currently estimated to be around 256,000-512,000 samples—corresponding to about 32-64 μsec of captured data. A trigger signal input allows the receiver to estimate the time of arrival of received samples for ranging, and the ability to synchronize multiple receivers to a common clock signal allows for precise position location.

Accomplishments during reporting period: Several provisions for integrating the software radio into the AWINN activities have been included in the design of both the prototype and full receiver. To facilitate synchronization of several receivers, the clock distribution network was modified to allow for several receivers to be synchronized to a single clock source. A trigger signal input allows the receiver to operate in the data capture mode and measure the time of

arrival for UWB pulses. Finally, FPGA code for the data capture mode is under development and will be implemented on the prototype receiver board.

Schedule:
- Summer 2005 – Evaluate Prototype Receiver
  - Verify the Receiver Operates in All Modes
  - Verify FPGA Code for Data Capture as well as PowerPC Processing
- Fall 2005 – Refine FPGA/PowerPC code for ranging and/or position location
  - Support Code Development with Measurements either from Lab Equipment or the Prototype Reciever
- Spring 2006 – Integrate Full Receiver into AWINN Activities
  - Crane Demonstration
  - Position Location
  - Imaging
  - Channel Measurements

Personnel:
    Chris R. Anderson – Transmitter and Receiver Hardware Development
    Deepak Agarwal – Receiver FPGA Code Development

Subtask 1.2f UWB applications to technology development applicable to Sea-Basing: position location, ranging, and imaging.

Task objective: The objective of this subtask is to develop algorithms that allow UWB technology to provide precision position location, precision ranging, and imaging. With a low duty cycle and wide bandwidth, UWB is naturally suitable to radar and ranging applications. As the time duration of a pulse decreases, it provides finer resolution of reflected signals, such that the system can resolve distances with sub-centimeter accuracy using simple signal processing algorithms.

For ranging applications, the focus of this subtask will be supporting the ship-to-ship crane cargo transfer. To determine the distance of a cargo container above a ships deck, multiple antennas will be attached to the four bottom corners of the cargo container. By operating the antennas as transmitter-receiver pairs in a round-robin fashion, the time-of-flight for a UWB pulse to be launched from the transmitter antenna, reflect off the ships deck, and arrive at the receive antenna can be measured. Using simple geometry, the height above the ships deck can be calculated, as illustrated in Figure 1.2-12. By combining range information from each pair of antennas (the front, the right and left sides, and the back), the 3-Dimentional position of the cargo container above the ship's deck can be calculated.
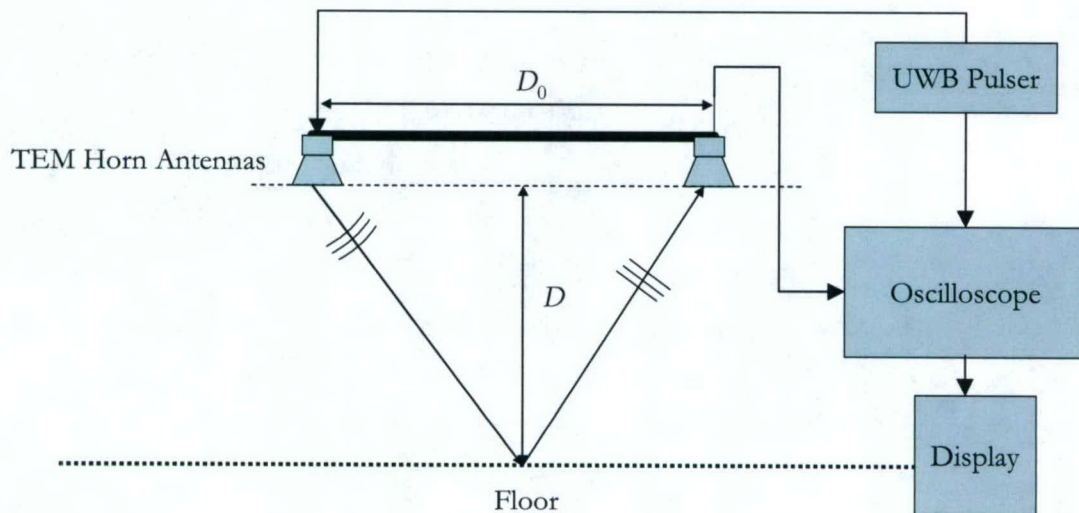
Figure 1.2-12 Illustration of the Crane Cargo Ranging Setup. The Time-of-flight from the transmitter to the receiver antenna can be measured, and since D_0 is known, the height above the deck, D, can be calculated.

Position location using UWB signals can be accomplished both passively and actively. Active position location using UWB is similar to standard TOA or TDOA techniques currently used commercially as well as in the military. The ability of UWB pulses to precisely resolve multipath signals in the environment, however, allows for passive position location. For example, inserting an object into an environment will create a resolvable multipath signal. If the transmitter and receiver positions are precisely known, then the location of the reflected signal can be constrained to be on an ellipse, where the transmitter and receiver are the foci, as shown in Figure 1.2-13. Combining results from multiple transmitter-receiver pairs will allow for the construction of multiple ellipses. The point at which these ellipses intersect will determine the position of the object.

Figure 1.2-13 Illustration of passive position location using UWB signals. The actual object position is given by the star symbol. The point where the two ellipses intersect is the calculated position of the object.
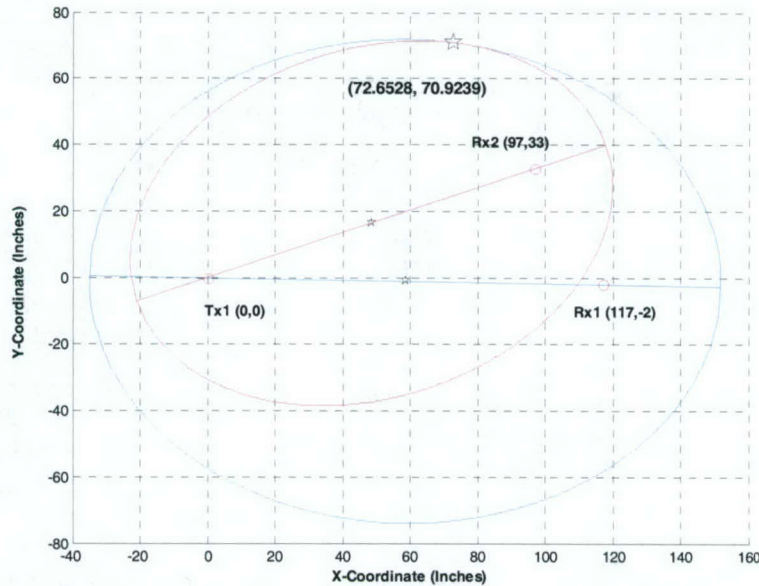
Accomplishments during reporting period: Initial experiments have been performed to demonstrate a proof-of-concept for the ranging and position location algorithms. For the ranging algorithm, a simple test rig was created where two antennas were attached to the ends of a metal rod. The rod was suspended from the ceiling in such a way that its height above ground could be varied. Using an oscilloscope and a laptop computer, the time-of-flight of a UWB pulse was measured, and the height above the floor was calculated for several positions. The measurement results (shown below in Table 1) indicate ranging accuracy on the order of an inch.

Table 1.2-1 Initial Ranging Experiment Results		
Position Number	Actual Range (ft)	Estimated Range (ft)
1	3.3	3.4
2	4.5	4.4
3	5.0	5.1
4	6.1	6.1
5	6.7	6.6

For the position location experiment, a set of five metallic reflectors were place in a straight line approximately six inches apart. A series of multipath delay profile measurements were then recorded at multiple transmitter-receiver locations. A Matlab post-processing routine was then able to generate a series of ellipses for each transmitter-receiver pair and then compute the probable location of each metallic reflector. Results are shown in Figure 1.2-14.

24
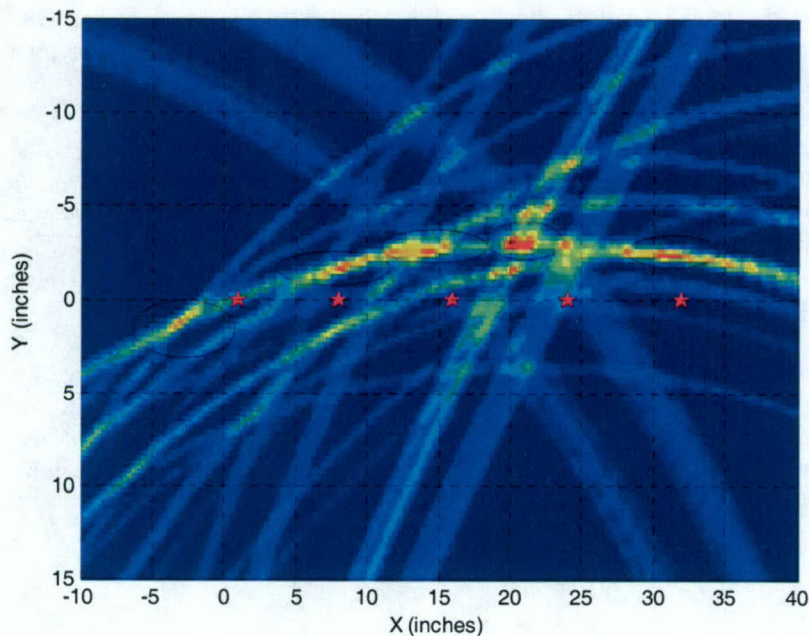
Figure 1.2-14 Initial position location experiment results. The actual object positions are given by the star symbols. The points where the ellipses intersect are the calculated positions of the objects.

Schedule:
- January-Summer 2005
  - Begin algorithm development
  - Test algorithms using the simple setups discussed above
- Summer-Fall 2005
  - Integrate ranging system into the crane hardware
  - Evaluate performance of position location algorithms in real-world environments
- January-Summer 2006
  - Finalize 3-D Ranging solution
  - Demonstrate passive and active position location system in laboratory environment.

Personnel:
Swaroop Venkatesh – Position Location Algorithm Development

1.2.3 Importance/Relevance

The simulation results from the SDR testbed simulations demonstrate that the time-interleaved sampling approach is a viable hardware architecture. The use of TI-Sampling with digital demodulation provides a tremendous amount of flexibility in the receiver operation. Even though the receiver is optimized for impulse UWB communication, it should be capable of using almost any broadband communication scheme.

The UWB SDR algorithm design is investigating ways of improving signal acquisition and tracking, as well as operation in multipath environments. The ship-based environment tends to

25

generate a large number of multipath signals, which represent a tremendous amount of energy available for the receiver to capture. Using a pilot-based matched filter topology, the receiver can capture a large percentage of the available energy without resorting to the complex tracking algorithms required by Rake receivers.

The distributed MIMO architecture investigated in this task will allow a number of UAVs to coordinate their transmissions and take advantage of space-time coding performance gains. These performance gains are available even if the various UAVs are not perfectly synchronized— an important consideration if the transmission involves a UWB signal. Combining UWB with distributed MIMO, we believe that long-range transmissions should be possible while still maintaining the LPI properties of UWB signals.

Finally, UWB signals have been demonstrated to have precision ranging and position location properties. Combining 3D ranging information with the crane control system should allow for sea-based ship-ship cargo transfer. Additionally, the position location abilities of UWB will allow for inventory control and tracking, as well as the precision maneuvering required to establish the ship-ship cargo transfer.

1.2.4 Productivity

Students supported
    Chris R. Anderson, Jan. 15, 2005 – present
    Jihad Ibrahim, Jan. 15, 2005 – present
    Swaroop Venkatesh, Jan. 15, 2005 – present
    Maruf Mohammad, Jan. 15, 2005 – present

Faculty supported
    Jeffrey H. Reed, Jan. 15, 2005 – present
    R. Michael Buehrer, Jan. 15, 2005 – present
    William H. Tranter, Jan. 15, 2005 – present

Papers Published
1. J. Ibrahim and R.M. Buehrer, " Two-Stage Acquisition for UWB in Dense Multipath," submitted to *IEEE Journal on Selected Areas in Communications*, March 2005.

1.3 Task 1.3 Collaborative and Secure Wireless Communications

1.3.1 Overview

Task Goal: We will investigate improving the communication link performance between a (mobile) base station and a spatially distributed, mobile, sensor network, exploiting collaborative network features.

Specifically, we will exploit the collective behavior of the sensor network to solve specific communications problems collaboratively. Utilizing emerging run-time reconfigurable computing technology, the radio infrastructure of a compact sensing node (fixed, mobile, floating, airborne, or submerged) can satisfy the diverse communications modes without a sizable impact on size, weight or power. By expanding this nodal capability to a network of autonomous sensing platforms, new opportunities for communications and computing research can be created that directly benefit the overall communications infrastructure. We will research and demonstrate collaborative communication techniques for remote sensing applications. We will investigate link-level strategies in which a network of sensing vehicles can be exploited to improve link performance. We will develop a communication scheme for inter-sensor message passing. The investigators, in collaboration with Task 1.1 and Task 1.2, will implement and characterize a node-to-node link. We will deploy hardware encryption for the protection of sensor intellectual property. In cooperation with the investigators of Task 1.1 on antenna integration and Task 1.2 on SDR integration, we will implement sensor-to-sensor link, sensor-to-base station link, and possibly sensor-to-GEO link (GPS). A multi-mode transceiver will be developed to satisfy (a) communications between network members, (b) communications with the ground-station, and (c) communications with external factors, such as GPS. We will work with the investigators of Task 2.1 to use a sensor network as a deployable ad-hoc network. We will support the AWINN integration, including ground-based demonstration of a mobile sensor network system.

Organization and Personnel: This task is managed by Directors of Virginia Tech Configurable Computing Lab using the following personnel:

Peter Athanas, Co-Director
Mark Jones, Co-Director
Deepak Agarwal, GRA
Brian Marshall, GRA

Summary: Effort this first quarter was directed towards Subtasks 1.3a and 1.3b. This section summarizes the activities on these two tasks over the past quarter.

- Simulation of collaborative methods (Subtask 1.3a)

The objective of Task 1.3a is to simulate collaborative methods using a network of sensor platforms. To accomplish this, a distributed control system for mobile, autonomous robot surveillance based on the principles of swarm intelligence was created. The system's goal is to locate and gather information from mobile targets in an unknown and possibly harsh environment. Swarm Intelligence uses the cooperation of multiple agents with limited local knowledge to accomplish a global task. Swarms have no centralized controlling agent, which is particularly useful in a harsh environment. Any robotic agent can be destroyed and the system remains capable of accomplishing its goals. Also due to the agents' simplicity, their cost will be lower.

Many researchers have previously used swarm intelligent systems to accomplish resource-gathering tasks such as defusing mines. Surveillance is basically a resource-gathering task where information is the resource. The autonomous agents in a swarm intelligent system use information from the local environment and communication from other agents to switch between behavior "states", for example *searching* or *following signal*. In current research reviewed, all communication from other robots is assumed to be truthful and agents blindly switch states based upon it. What happens if one of the robotic agents malfunctions or the communication signal protocol is compromised by a malicious force? This could result in a traffic jam like situation causing the whole system to enter a deadlock state. For example, if one robot continually calls others to its location and they blindly follow that signal, eventually all the robots will uselessly congregate in one area.

In an effort to address this, a first generation simulator has been constructed that implements a threshold between state changes based on knowledge gained locally. Instead of blindly changing states, the agents may ignore external communication based on their internal knowledge such as message duration, location within the area, and local sensor input. This will eliminate the domino effect caused by erroneous communication as described above. Also, this threshold can be used to control the size and density of a swarm. For example, the agent may ignore a call from another agent if it has already detected many other agents in that area.

Due to the time and physical space requirement of running tests in hardware, we decided a simulator was necessary to properly analyze the effect of changing parameters within the control system. After surveying possible simulation packages, we settled on StarLOGO as the software program to model the ER1 robotic hardware. StarLOGO is a free software package from MIT designed specifically for experiments into swarm intelligence. We have a developed a simulation of the surveillance system to test various situations and performance parameters, such as broadcast and sensor ranges.

The robotic hardware used for the system is manufactured by Evolution Robotics. The ER1 Personal Robotic System uses any laptop for controlling the drive motors, IR sensors, and image recognition. The control algorithms are currently being implemented on this hardware platform and should soon be completed.

Preliminary simulation results have been obtained, and were presented at the kick-off meeting in April.

- Demonstration and characterization of a link between multiple nodes (Subtask 1.3b)

The aim of this task is to build an impulse-based ultra wideband communication system testbed that will allow researchers to evaluate different UWB modulation, multiple access, and coding schemes, and will support raw data rates of up to 100 MB/s. The transceiver is being developed using software/reconfigurable radio concepts and will be implemented using commercially available off-the-shelf components. The heart and soul of an SDR UWB transceiver is the digital processing hardware, which must be capable of handling high-speed data streams from the Analog to Digital Converters (ADCs) and then process the data in real time. A high performance Xilinx Virtex-II Pro (XC2VP70) FPGA was chosen for this task. In addition to providing a large amount of reconfigurable logic resources—these are capable of supporting multiple I/O standards, have large number of available user I/O pins, and have embedded processor cores. The testbed has two components: a non-real time part for data capture and signal acquisition, and a real-time part for data demodulation and signal processing. The non-real time component uses the internal Block RAMs to store a set of samples and one of the PowerPC cores to process the data offline, to minimize logic resource usage. The real-time part uses distributed memory to store incoming data and processes it using hardwired multipliers and FPGA logic cells.
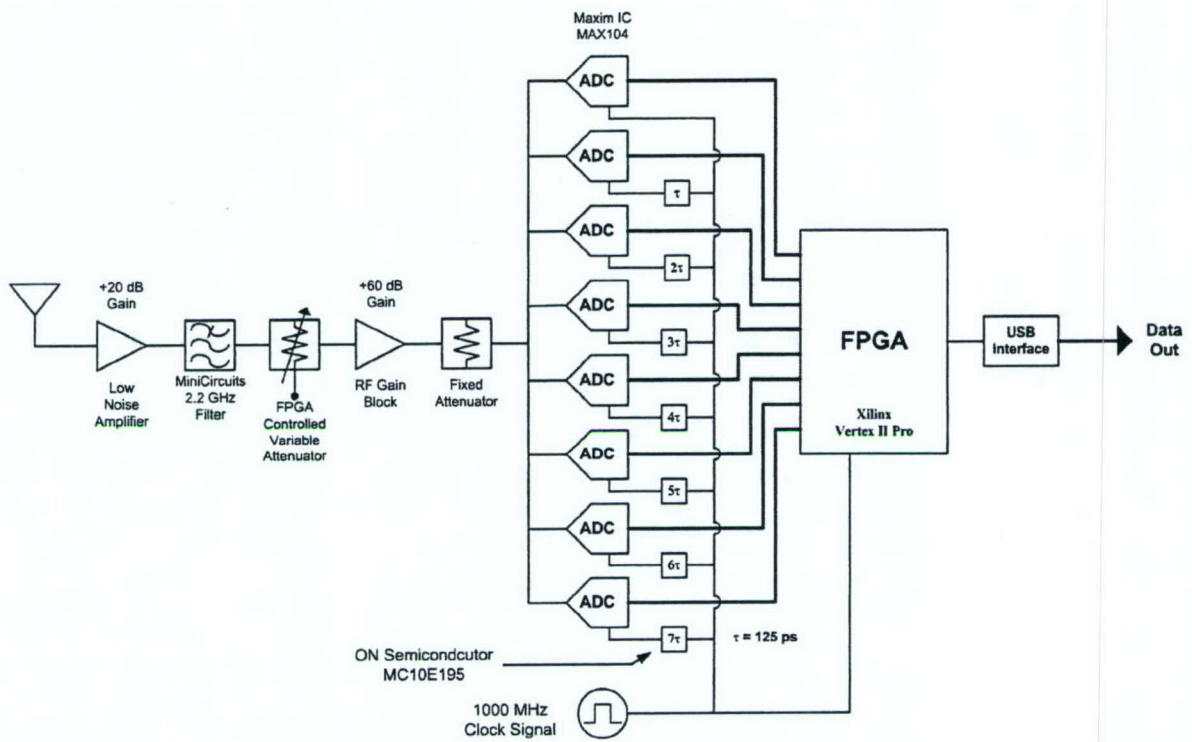
Figure 1.3-1 Block diagram of the software-defined ultra wideband communication system.
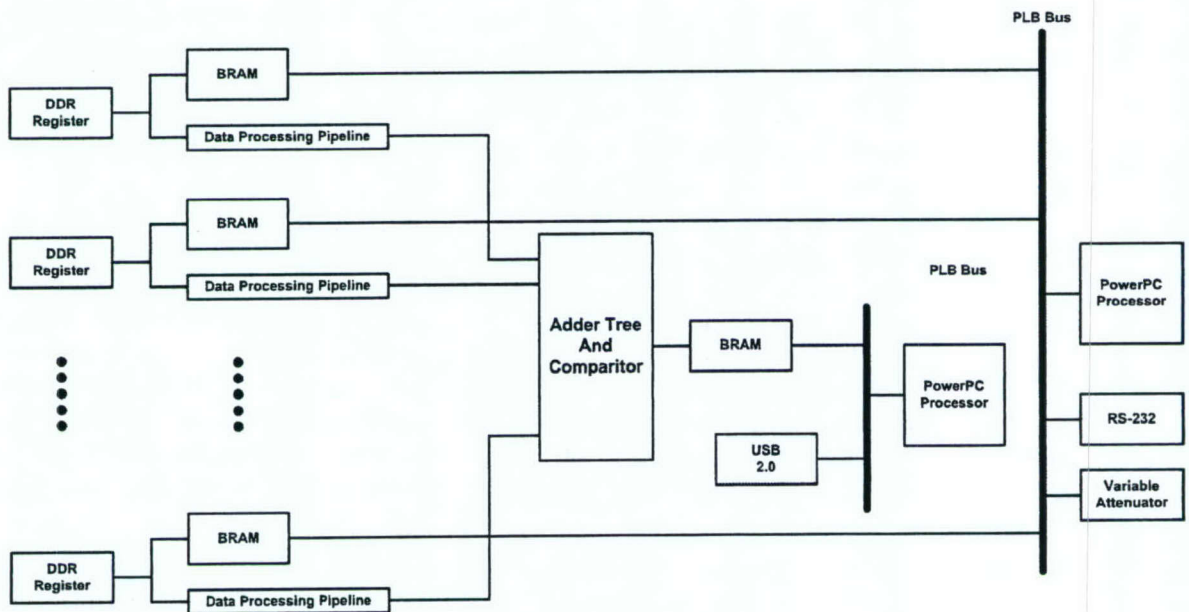

Figure 1.3-2 Block diagram of the digital processing hardware for the UWB communication system.

A Software Defined Radio UWB receiver provides tremendous flexibility and rapid prototyping capabilities over a fixed hardware implementation. Such a receiver has the capability of supporting multiple data rates, modulation or multiple access schemes, and can adapt to the propagation environment. Currently, state-of-the-art UWB communication systems are composed of custom-developed hardware, and do not use SDR architectures. The challenges involved in developing such as communication testbed—extremely high sampling rates, huge amounts of input/output data, and a tremendous amount of digital processing power—have been fairly daunting. These challenges become particularly poignant when Commercially available Off-The-Shelf (COTS) components are used in the development of such a system. The communication system was designed to operate at a data rate of 100 Mbps, to utilize any of the two popular UWB modulation schemes (Pulse Position or Pulse Amplitude), and to support a variety of multiple access or coding schemes.

This quarter's effort was directed towards freezing the architecture of the SDR receiver and a number of designs, experiments and analysis was performed to achieve this. Because a UWB 500-picosecond pulse width is used in the communication system, accurately reconstructing it in the digital domain requires a sampling rate of 8 GHz. A Time-Interleaved Sampling (TI-Sampling) approach—where multiple ADCs sample the received signal at different points in time in a round-robin fashion —was used to achieve the target sampling frequency. TI-Sampling is advantageous in a COTS implementation as it significantly relaxes the requirements on the interface between the ADCs and the FPGA while still preserving the quality of the received signal.

The MAX104 ADCs used in the design have an integrated demultiplexer that produces samples on a primary and auxiliary buss, each operating at half the sampling frequency (i.e. 500 MHz). To input data at such high speeds, the FPGA uses LVDS extended IO standard and Double Data Rate (DDR) Registers operating at half the clock frequency (i.e. 250 MHz). Matched filtering is performed by multiplying and integrating the received pulse with the template waveform, and then comparing the result to the receiver decision statistic threshold. To achieve real time processing of the input samples, similar high speed datapaths clocked at 250 MHz were implemented for each DDR register. These datapaths mainly consist of adders, multipliers and multiplexers and are heavily pipelined to allow the synthesis tools to perform register balancing and other optimizations.

The FPGA receives eight pairs of data busses (primary and auxiliary buss from an ADC) clocked at 500 MHz. Each clock will have a dedicated DCM that will de-skew the clock and phase shift it to align it with the incoming data. The CLKIN_DIV_BY_2 attribute will be used to divide the incoming clock to 250 MHz. Each DCM produces 2 clock outputs (Clk0 and Clk180), yielding a total of 16 local clocks in the FPGA. Timing closure for this design is difficult to achieve because of the presence of large number of clocks in the design and the tight timing constraints. FPGA floorplanning was performed and additional timing constraints used to achieve the target clock period of 3.9 ns (4 ns clock cycle with an allowance of 100 ps for DCM clock jitter).

To correct the effects of a one or two sample random timing jitter—as well as to maintain synchronization between Users—an early-late algorithm is implemented. The receiver performs matched filter coefficient with three template waveforms generated as follows:

1. One template advanced in time by one sample

2. One template with ideal timing

3. One template delayed in time by one sample

The template waveform registers are connected in the form of circular shift register chains, and in case the late or early templates give a stronger correlation, the shift registers are advanced or delayed by one to correct the timing error.
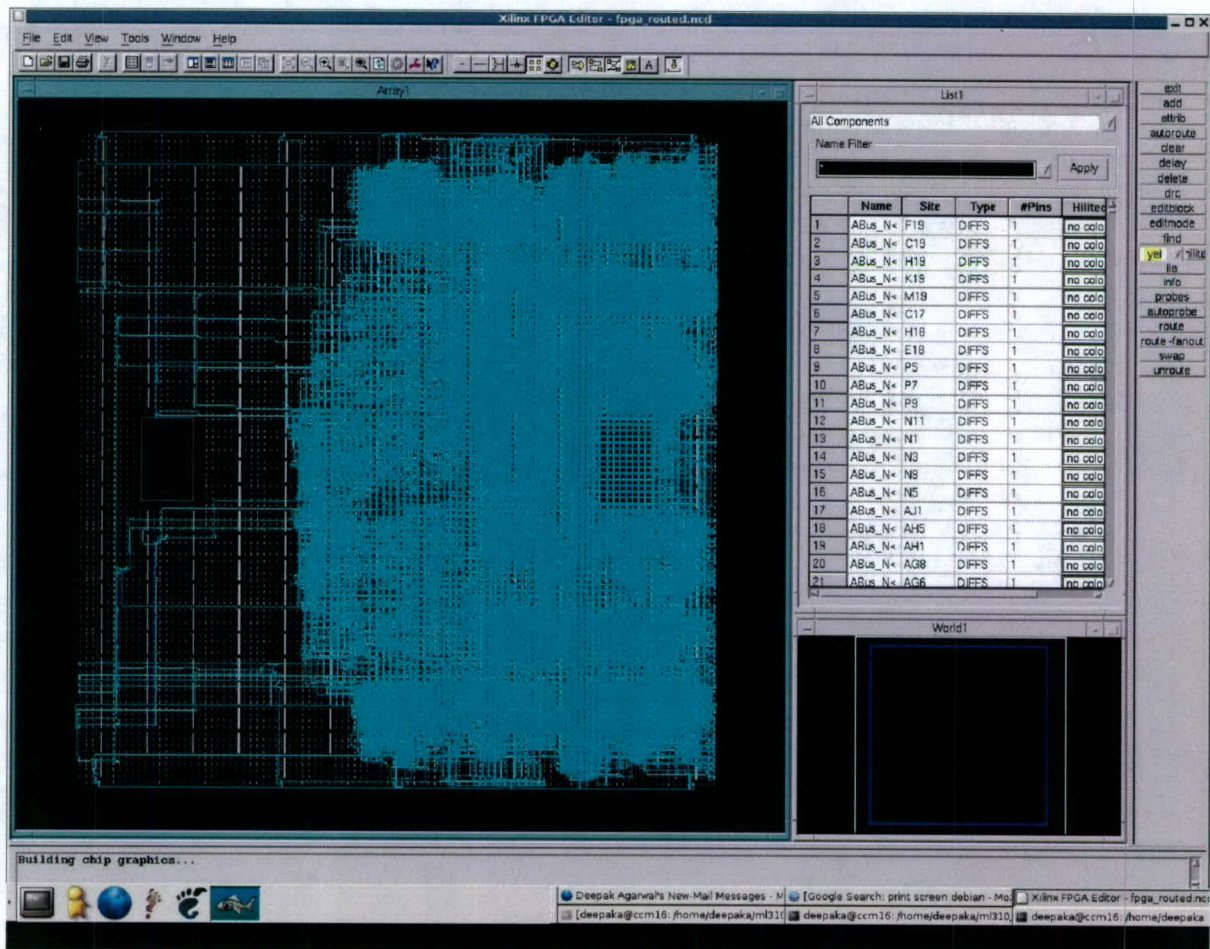
Figure 1.3-3 FPGA editor snapshot of the partial SDR receiver design with 250 MHz datapaths for data demodulation and real-time tracking. It uses 23% of the FPGA slices.

Due to analog RF constraints, all of the ADCs busses are connected to IOBs on only two quadrants of the FPGA. This severely restrains the IO placement for the FPGA because of the routing congestion caused by the limited availability of routing layers and pins. This was a design issue which affected all aspects of PCB and FPGA design and had to be resolved before we could make any progress with the actual designs. Hence pin placements for all the 256 data pins were fixed and routing layers assigned to make sure we do not end up with an un-routable PCB Board.

To establish the communication link, User 1 broadcasts an acquisition signal, which consists of N UWB pulses that are amplitude modulated by a maximal-length sequence (m-sequence), followed by an N pulse long period of no signal transmission. User 1 will continue broadcasting the acquisition sequence until it receives an acknowledgement signal from the receiver User 2.

31

To acquire the transmitted signal, the FPGA in User 2's receiver will capture a set of samples equal to 3N UWB pulses and store them in BRAMs. Each DDR register is associated with a 16kB dual port BRAM, one port of which can be accessed by the DDR register, and the other port is mapped to the PLB bus on one of the FPGA's PowerPC processors. Capturing 3N samples guarantees that at least one complete m-sequence will be captured. Control is then passed to the embedded PowerPC processor.

The PowerPC processor performs a sliding correlation operation using a stored template waveform. While the sliding correlation operation is being performed, the sample values stored in BRAMs do not change. A 32-bit counter keeps track of number of samples that have been skipped. The strongest correlation will occur when the template waveform is precisely aligned to the received signal. The PowerPC processor can then calculate the point in time when it should receive the next m-sequence transmission.

Even though acquisition is performed in non-real time, the number of processing cycles that can be used is significantly restricted. Because the master oscillators for User 1 and User 2 are not precisely synchronized, they may drift apart during acquisition. The drift creates a window of uncertainty about the calculated start time of the next m-sequence. Experimentally, it was determined that the maximum uncertainty window that could be tolerated was half the number of samples in a UWB pulse (i.e. 40 samples). The master oscillators on the transceiver have a frequency of 1 GHz and a stability of ±20 parts per million (ppm). Thus, the maximum allowable acquisition time is 1 ms. The PowerPC processor operates at frequency of 300 MHz. An acquisition time of 1 ms gives the receiver 333,000 processor cycles to complete the first stage of acquisition. This is a hard restriction which determines the length of m-sequence that can be used for the acquisition. The software routines for acquisition were written, and the equivalent PowerPC assembly generated and optimized to reduce the number of clock cycles for each of the iterations to 25 for the innermost loop in the calculations. M-sequences are only of length $N = 2r - 1$, hence N can be (3, 7, 15, 31 ...). A $N=7$ M-sequence requires 294,000 processor cycles, whereas an $N=15$ m-sequence requires 630,000 processor cycles. Thus, $N=7$ was chosen. A number of detection test runs were performed with sample data sets to make sure this is sufficient for detecting a UWB pulse.

1.3.2 Task Activities for the Period

Subtask 1.3a Simulation of collaborative methods on a network of sensor platforms using data collected from laboratory prototypes.

Accomplishments during reporting period:
1. Background literature review conducted.

2. First version of the simulator created based on StarLOGO.

3. Preliminary results obtained that are currently being analyzed.

Links to other tasks: This is prerequisite work for Subtasks 1.3c, 1.3e, and 1.3f.
Schedule: This will continue throughout Year 1.
Personnel: Brian Marshall, GRA

Subtask 1.3b Demonstration and characterization of an inter-sensor link between two or more (mobile) nodes, including a low-power UWB communication scheme for inter-sensor messaging.

Accomplishments during reporting period:

1. Finalized the architecture of the SDR receiver including the clocking scheme, FPGA pins and part placement and hardware-software partitioning for the FPGA.

2. The acquisition and synchronization schemes were finalized based on the restrictions imposed by the embedded PowerPC Processor

3. Partial designs for the SDR Receiver were done to ensure the feasibility of implementing datapath capable of processing 64 Gbps data rate.

4. The design for a prototype SDR receiver that will serve as a testing and development platform for the UWB transceiver was finalized.

Links to other tasks: This is prerequisite work for Subtasks 1.3c, 1.3d, and 1.3f.
Schedule: This will continue throughout Year 1.
Personnel: Deepak Agarwal, GRA

Subtask 1.3c In cooperation with Tasks 1.1 and 1.2, implement and characterize a node-to-node link.

This task has not started. This task depends upon Subtasks 1.3a and 1.3b.

Subtask 1.3d Create two or more multi-mode radio prototypes that can be deployed in a meaningful way on the campus to demonstrate the communications modes.

This task has not been started.

Subtask 1.3e In cooperation with Task 2.1, perform a simulation that illustrates the network being transformed into an ad hoc network using a node model.

This task has not been started.

Subtask 1.3f Demonstrate a multi-node system comprised of commodity robotic devices to emulate behavior of a loosely coupled mobile sensor network.

This task has not been started.

1.3.3 Importance/Relevance

Software defined radios have the potential of changing the fundamental usage model of wireless communications devices, but the capabilities of these transceivers are often limited by the speed of the underlying processors. Here we make an attempt to solve this problem by using reconfigurable architectures to develop custom datapaths which can handle these high data rates using commercially available FPGAs as an alternative to custom ASICs which lead to the obvious cost and development time benefits. An added advantage of such architecture is the capability to use run-time reconfigurablity to adapt to the effects of pulse shaping, channel coding, error control, and network algorithms on UWB communication. It can also be used to implement advanced cryptosystems or obfuscate communication.

1.3.4 Productivity

Conference publications
D. Agarwal, P. Athanas, "An 8 GHz UWB Transceiver Prototyping Testbed," IEEE International Rapid Systems Prototyping Conference, (Montreal, Canada) June 8-12, 2005.

Students supported
    Deepak Agarwal: 2/2005 - present

2. TASK 2 Secure and Robust Networks

2.1 Task 2.1 Ad Hoc Networks

2.1.1 Overview

Task Goal: This task investigate core network capabilities for quality of service (QoS), security, and routing in ad hoc networks, especially mobile ad hoc networks (MANETs).

Organization: This task is managed by Scott Midkiff using the following personnel:
Scott F. Midkiff, task director
Luiz A. DaSilva, faculty
Nathaniel J. Davis, IV, faculty
Y. Thomas Hou, faculty
George Hadjichristofi, GRA
Unghee Lee, GRA (33% for reporting period)

Summary: This quarter we focused on security mechanisms for ad hoc networks, combined routing and medium access control (MAC) protocols for ad hoc network, and planning test bed expansion. The accomplishments and other details are provided in Section 2.1.2 below.

2.1.2 Task Activities for the Period

Subtask 2.1a Policy-based Quality of Service

Task Objective: The objectives of this subtask are to investigate and develop quality of service mechanisms that provide differential bandwidth allocation and scheduling based on traffic type, node type, and the current network environment. We seek to increase the adaptability of the QoS mechanisms to operate more robustly in a variety of environments. We will also explores automatic adaptation at the physical and data link layers in response to application and network-layer demands, as an initial exploration of cognitive networks as an approach to cross-layer optimization.

Accomplishments during reporting period: Minimal activities pertaining to this subtask took place during the reporting period.

Links to other tasks: This subtask has natural synergies with Task 2.4 (Cross-Layer Optimization), as the mechanisms that support QoS in mobile ad hoc networks span the physical, data link, network and application layers. It also integrates with Task 2.2 (Real-Time Resource Management, Communication, and Middleware) as some of the QoS mechanisms developed here will support real-time applications and must integrate with the real-time middleware developed in Task 2.2.

Schedule: The schedule for this subtask is as follows.
- Develop extended policy-based QoS mechanism (April-June 2005)
- Explore adaptability methods (July-December 2005)
- Integrate cross-layer design features (July-September 2005)
- Realize prototype implementation (July-December 2005)
- Integrate protocols using test bed (January-March 2006)
- Refine protocols based on performance evaluation and demonstrations (April-June 2006)

Personnel: The following personnel were assigned to this subtask.
    Luiz A. DaSilva, faculty
    Scott F. Midkiff, faculty

Subtask 2.1b Security Mechanisms for Ad Hoc Environments

Task Objective: The objectives of this subtask are to investigate and, where feasible and deemed appropriate, develop security mechanisms that are efficient for ad hoc network environments. Our initial emphasis will consider a distributed key management system (KMS) and associated shared trust schemes.

Accomplishments during reporting period: Activities focused on further development of a distributed certificate authority (DCA) and trust management scheme. Performance results were obtained using a customized simulator. The scheme utilizes a control plane of certificate authorities (CAs) and trusted peers. This increases security service availability for mobile nodes and is at the top of the pyramid shown in Figure 2.1-1 as it directly offers capabilities to network nodes. Distributed CAs (DCAs) can be loaded offline from a root CA. If a DCA is not available, then a temporary CA (TCA) can be established using a node that has previously obtained a certificate of interest from a DCA. Finally, peer-to-peer trust can be established. Different levels of security should be associated with these three levels of authentication and trust.

Trust with peers implies the use of a behavior grading scheme for key management, which is at the center of the pyramid shown in Figure 2.1-1. At the bottom of there pyramid there is an intrusion detection system (IDS) that grades overall trust in the network.

The concept of behavior grading – at the local peer and network levels – is particularly important as it is integrated with the key management system to control functions such as revocation of a certificate.

Links to other tasks: This subtask has synergies with Subtask 2.1c and Task 2.4 (Cross-Layer Optimization) as link layer and, especially, network layer information can be employed to improve key management and other security functions. We will deploy a prototype for evaluation in the test bed developed in Subtask 2.1d and use tools of Subtask 2.1e.

Schedule: The schedule for this subtask is as follows.
–   Develop DCA and trust management system (January-June 2005)
–   Integrate cross-layer design features (July-September 2005)
–   Realize prototype implementation (July-December 2005)
–   Integrate protocols using test bed (January-March 2006)
–   Refine protocols based on performance evaluation and demonstrations (April-June 2006)

Personnel: The following personnel were assigned to this subtask.
    Nathaniel J. Davis, IV, faculty
    Scott F. Midkiff, faculty
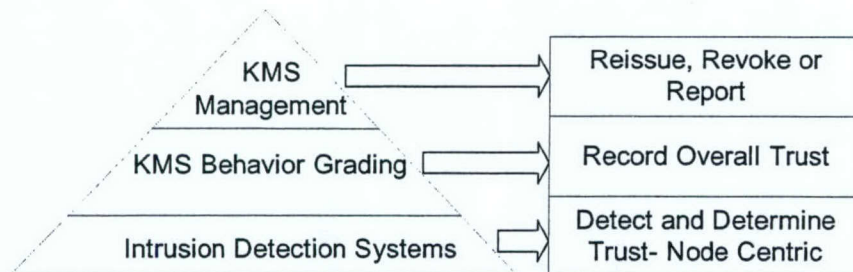   George Hadjichristofi, GRA

Figure 2.1-1 Illustration of tiers of a robust, secure scheme for key management and behavior grading.

Subtask 2.1c Ad Hoc Routing Optimization

Task Objective: The objectives of this subtask are to investigate schemes to improve routing and to use network layer functionality to improve other network services.

Accomplishments during reporting period: During the current reporting period, our focus was on employing cross-layer design of the medium access control and routing layers. In particular, we extended the design of the Destination-Sequenced Distance-Vector (DSDV) proactive MANET routing protocol to enable use of multiple channels at the MAC layer. The new protocol, DSDV for Multiple Channels (DSDV-MC) has been designed and simulated using the ns2 simulation environment. We also began work on extending the Open Shortest Path First with Minimum Connected Dominating Sets (OSPF-MCDS) MANET routing protocol to support multiple channels. We also developed specific design principles to guide this and related research (see Gong and Midkiff, 2005).

Some illustrative initial results for a mobile, multi-hop ad hoc network are shown in Figures 2.1-2 and Figures 2.1-3. Figure 2.1-2 compares the goodput (useful throughput) of a baseline case of using DSDV over a single channel with using DSDV-MC for 3 to 11 different channels. The results show that using multiple channels can substantially increase network goodput. Figure 2.1-3 compares the routing overhead for DSDV versus DSDV-MC for 3 to 11 channels. While there is some increase in overhead due to DSDV-MC, the increase is relatively modest.

Links to other tasks: This subtask has direct ties to Task 2.4 (Cross-Layer Optimization) as our focus makes the network layer a key part of our cross-layer optimization schemes. In addition, we will explore synergy with Task 2.2 (Real-Time Resource Management, Communication, and Middleware). We will deploy a prototype for evaluation in the test bed developed in Subtask 2.1d and use tools of Subtask 2.1e.

Schedule: The schedule is as follows.
- Extend DSDV to support multichannel MAC (January-March 2005)
- Extend OSPF-MCDS to support multichannel MAC (April-June 2005)
- Extend Optimized Link State Routing (OLSR) to support (July-September 2005)
- Realized prototype implementation in Linux (July-September 2005)
- Provide enhanced support for policy-based network management (PBNM) (July-September 2005)
- Provide enhanced support for security services (October-December 2005)
- Integrate additional cross-layer enhancements (October-December 2005)
- Integrate protocols using test bed (January-March 2006)

37

– Refine protocols based on performance evaluation and demonstrations (April-June 2006)

Personnel: The following personnel were assigned to this subtask.
Scott F. Midkiff, faculty
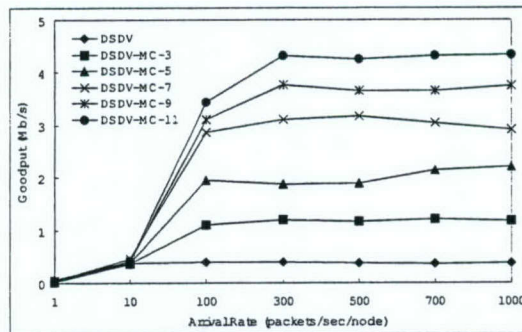Unghee Lee, GRA (33%)

Figure 2.1-2 Goodput for a multi-hop mobile network for a varying packet arrival rate.
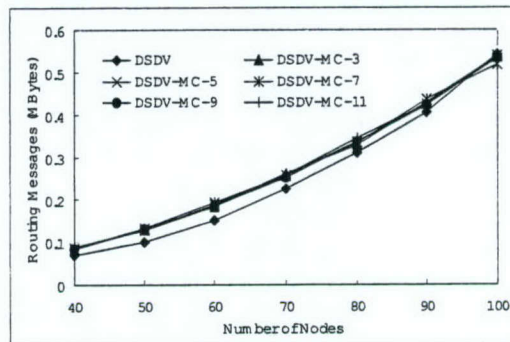

Figure 2.1-3 Routing overhead for a multi-hop mobile network for a varying number of nodes.

Subtask 2.1d Test Bed Evaluation and Demonstration

Task Objective: The objectives of this subtask are to integrate and demonstrate through research prototype implementations key ideas from Subtasks 2.1(a), 2.1(b), and 2.1(c) and, as feasible and appropriate, from Task 2.2 (Real-Time Resource Management, Communication, and Middleware), Task 2.3 (Network Interoperability and Quality of Service), and Task 2.4 (Cross-Layer Optimization). The objective includes exploring interactions between different components and functions and to evaluate and demonstrate both functionality and performance.

Accomplishments during reporting period: There were no activities for this subtask in the reporting period.

Links to other tasks: The test bed evaluation and demonstrations rely on results from Subtasks 2.1a, 2.1b, and 2.1c, as well as Tasks 2.2, 2.3, and 2.4.

Schedule: The schedule for this subtask is as follows.
– Identify and clarify needs (July-September 2005)
– Acquire and deploy test bed hardware (October-December 2005)
– Deploy technologies in test bed (January-March 2006)
– Final performance evaluation and demonstrations (April-June 2006)

38

Personnel: No personnel were assigned to this subtask for the reporting period.

Subtask 2.1e Configuration and Monitoring Tools

Task Objective: The objectives of this subtask are to investigate and develop software configuration and monitoring tools to facilitate network testing and demonstration.

Accomplishments during reporting period: There were no activities for this subtask in the reporting period.

Links to other tasks: The tools support the test bed described above for Subtask 2.1(d).

Schedule: The schedule for this subtask is as follows.
- Identify and clarify needs (April-June 2005)
- Implement and test tools (July-December 2005)
- Utilization and refinement of tools (January-June 2006)

Personnel: No personnel were assigned to this subtask for the reporting period.

2.1.3 Importance/Relevance

Ad hoc networks are of particular importance to the Navy and other DoD units because of their ability to be quickly configured and operate without infrastructure. Research in ad hoc networks to date has been dominated by solutions to particular, specific problems and not to general system and network infrastructure issues. This task focuses on making ad hoc network operate successfully as a system with efficient routing, the ability to offer quality of service, and the robustness and security required of military networks.

We presented this work to personnel from the Office of Naval Research and the Naval Research Laboratory (NRL) as part of the AWINN kickoff meeting on March 31, 2005 in Blacksburg, VA. Based on this meeting, we are working toward additional information sharing between our team and NRL personnel.

2.1.4 Productivity

Conference publications
  1. M. X. Gong and S. F. Midkiff, "Distributed Channel Assignment Protocols: A Cross-Layer Approach," *Proceedings IEEE Wireless Communications and Networking Conference* (WCNC), New Orleans, LA, March 13-17, 2005, 6 pages.

Students supported
  George Hadjichristofi, Jan. 15, 2005–present
  Unghee Lee, Jan. 15, 2005–present (33%)

Faculty supported
  Scott F. Midkiff, Jan. 15, 2005–present
  Luiz A. DaSilva, Jan. 15, 2005–present

2.2 Task 2.2 Real-Time Resource Management, Communications, and Middleware

This report discusses the progress of Task 2.2 during the first quarter - January through March, 2005. The report has four sections: (1) task overview, (2) task activities for the period, (3) importance to the Navy, and (4) productivity.

2.2.1 Task Overview

Task Goal: The goals of Task 2.2 include:

1. Develop time/utility function (TUF)/utility accrual (UA) scheduling algorithms for scheduling Real-Time CORBA 1.2's distributable threads with *assured timeliness properties* under failures. Develop distributable thread maintenance and recovery (TMAR) protocols that are integrated with such scheduling algorithms.

2. Develop TUF/UA *non-blocking synchronization mechanisms* for synchronizing distributable threads and single-processor threads for concurrently and mutually exclusively accessing shared objects.

3. Investigate how TUF/UA scheduling algorithms, synchronization mechanisms, and TMAR protocols can co-reside with policy-based network QoS management schemes, and jointly optimize (with network QoS schemes) UA timeliness optimality criteria, as envisaged in Task 2.3.

4. Develop the *Distributed Real-Time Specification for Java* (DRTSJ) standard under the auspices of Sun's Java Community Process (JCP)[1], incorporating scheduling algorithms, synchronization mechanisms, and TMAR protocols developed in (1) and (2).

Organization and Personnel:
  Dr. Binoy Ravindran, faculty and task director
  Jonathan Andersen, GRA
  Hyeonjoong Cho, GRA

Summary: Embedded real-time systems that are emerging such as control systems in the defense domain (e.g., Navy's DD(X), Air Force's AWACS) are fundamentally distinguished by the fact that they operate in environments with dynamically uncertain properties. These uncertainties include transient and sustained resource overloads due to context-dependent activity execution times and arbitrary activity arrival patterns. For example, many DoD combat systems include radar-based tracking subsystems that associate sensor reports to airborne object tracks. When significantly large number of sensor reports arrives, it exceeds the system processing capacity, causing overloads, resulting in important tracks to go undetected.

When resource overloads occur, meeting deadlines of all application activities is impossible as the demand exceeds the supply. The urgency of an activity is typically orthogonal to the relative importance of the activity—e.g., the most urgent activity can be the least important, and vice versa; the most urgent can be the most important, and vice versa. Hence, when overloads occur completing the most important activities irrespective of activity urgency is often desirable. Thus, a clear distinction has to be made between the urgency and the importance of activities during overloads. (During under-loads, such a distinction need not be made because deadline-based

---

[1] The DRTSJ effort is currently ongoing under a JCP called JSR-50. The core members of the DRTSJ team include those from The MITRE Corporation and Virginia Tech.

scheduling algorithms, such as EDF, are optimal for those situations [hor74]—i.e., they can satisfy all deadlines.)

Deadlines by themselves cannot express both urgency and importance. Thus, we consider the abstraction of time/utility functions (or TUFs) [jlt85] that express the utility of completing an application activity as a function of that activity's completion time. Utility is typically mapped to application-level quality of service (QoS) metrics such as track quality and track importance in a command and control application. We specify deadline as a binary-valued, downward "step" shaped TUF; Figure 2.2-1(a) shows examples. Note that a TUF decouples importance and urgency—i.e., urgency is measured as a deadline on the X-axis, and importance is denoted by utility on the Y-axis.
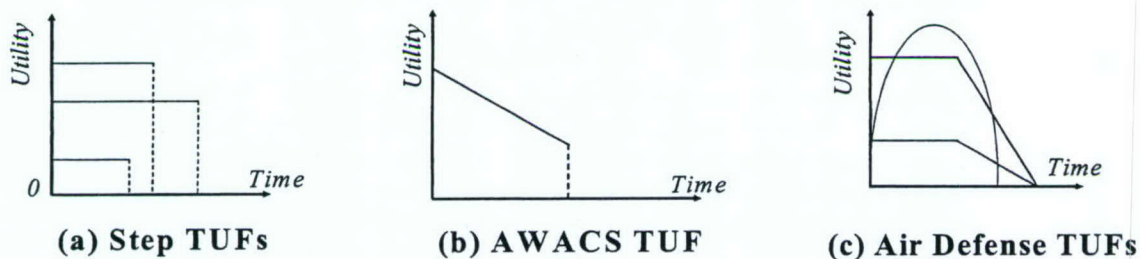

(a) Step TUFs   **(b) AWACS TUF**   **(c) Air Defense TUFs**

Figure 2.2-1 Example of timing requirements specified using time/utility functions.

Many embedded real-time systems also have activities that are subject to *non-deadline* time constraints, such as those where the utility attained for activity completion *varies* (e.g., decreases, increases) with completion time. This is in contrast to deadlines where a positive utility is accrued for completing the activity anytime before the deadline, after which zero or infinitively negative utility is accrued. Figures 2.2-1(b)—2.2-1(c) show examples of such time constraints for two real applications (see [cjk+99] and the references therein).

When activity time constraints are specified using TUFs which subsume deadlines, the scheduling criteria is based on accrued utility, such as maximizing the sum of the activities' attained utilities. We call such criteria, *utility accrual* (or UA) criteria, and scheduling algorithms that optimize them are called UA scheduling algorithms.

UA algorithms that maximize summed utility under downward step TUFs (or deadlines) [loc86, cla90, wrjb04] default to EDF during under-loads, because EDF can satisfy all deadlines during those situations. Consequently, they obtain the maximum total utility during under-loads. When overloads occur, they favor activities that are more important (since more utility can be attained from them), irrespective of their urgency. Thus, UA algorithms' timeliness behavior subsumes the optimal timeliness behavior of deadline scheduling.

The major Task 2.2 accomplishments of this quarter include development of UA algorithms that use *wait-free synchronization* for concurrently and mutually exclusively accessing shared data objects. We derived upper bounds on the maximum possible increase in activity utility that is possible with wait-free over their lock-based counterparts, while incurring the minimum possible additional space costs, and thereby establish the tradeoffs between wait-free and lock-based object sharing for UA scheduling. Our implementation measurements on a POSIX RTOS reveal that (during under-loads), the wait-free algorithms yield optimal utility for step TUFs and significantly higher utility (than lock-based) for non-step TUFs. We summarize this result in Section 2.2.2.

41

2.2.2 Task Activities for the Period

- Shared Data and Synchronization

Most embedded real-time systems involve mutually exclusive, concurrent access to shared data objects, resulting in contention for those objects. Resolution of the contention directly affects the system's timeliness, and thus the system's behavior. Mechanisms that resolve such contention can be broadly classified into: (1) lock-based schemes---e.g.,[srl90,cla90]; and (2) non-blocking schemes including wait-free protocols (e.g.,[kr93,cb97,hps02]) and lock-free protocols (e.g.,[arj97]).

Lock-based protocols have several disadvantages such as serialized access to shared objects, resulting in reduced concurrency and thus reduced resource utilization [arj97]. Further, many lock-based protocols typically incur additional run-time overhead due to protocol (or scheduler) activations that occur when activities request previously locked shared objects, which are scheduling events [srl90,cla90]. Another disadvantage is the possibility of deadlocks that can occur when lock holders crash, causing indefinite starvation to blockers. Further, many (real-time) lock-based protocols require a-priori knowledge of the ceilings of locks [srl90], which may be sometimes difficult to obtain. Furthermore, OS data structures (e.g., semaphore control blocks) must be a-priori updated with that knowledge, resulting in reduced flexibility [arj97].

These drawbacks have motivated research on wait-free object sharing in real-time systems. Wait-free protocols use multiple buffers (e.g., a circular buffer). For the single-writer/multiple-reader problem, wait-free protocols typically use buffers that is proportional to the maximum number of times the readers can be preempted by the writer, during when the readers are reading. The maximum number of preemptions of a reader by the writer bounds the number of times the writer can update the object while the reader is reading. Thus, by using as many buffers as the worst-case number of preemptions of readers by the writer, the readers and the writer can continuously read and write in different buffers, respectively, and thereby avoid interference.

However, wait-free protocols incur additional space costs due to their usage of multiple buffers, which is infeasible for many small-memory embedded real-time systems. Prior research has shown how to mitigate such costs. In [kr93], Kopetz et al. present one of the earliest wait-free protocols. Chen et al. build upon [kr93] and present an efficient wait-free protocol in [cb97]. Huang et al. improve the time costs of Chen's protocol in [hps02]. Chen's protocol is further improved by Cho et al. to develop the space-optimal wait-free protocol for the single-writer/multiple-reader problem in [crj05].

- Synchronization Under UA Scheduling

In this work, we consider wait-free synchronization for the single-writer/multiple-reader problem in embedded real-time systems that are subject to TUF time constraints and UA optimality criteria. Our motivation to consider wait-free synchronization for UA scheduling is to reap its advantages (e.g., reduced object access time, greater concurrency, reduced run-time overhead, fault-tolerance) toward better optimization of UA criteria. In particular, we hypothesize that the reduced shared object access time under wait-free synchronization will result in increased activity attained utility. Of course, this will come with the additional buffer cost.

Thus, our goal is to develop wait-free UA scheduling algorithms that use the absolute minimum buffer size, and verify whether such algorithms can yield greater activity utility than lock-based ones. This will allow us to establish the fundamental tradeoffs between wait-free and lock-based object sharing for UA scheduling. We precisely do so in this work.

We focus on wait-free synchronization, as opposed to lock-free, as lock-free incurs additional time costs (due to their retry loops), which can potentially reduce attained utility. We consider the single-writer/multiple-reader problem, as it occurs in most embedded real-time systems [hps02]. Further, we consider the UA optimality criteria of maximizing the sum of the activities' attained utilities, while yielding optimal total utility for step TUFs during under-loads, and ensuring the integrity of shared data objects under concurrent access.

UA scheduling under wait-free synchronization has never been studied in the past. Thus, we consider the two lock-based UA algorithms that match our exact UA criteria: (1) the Resource-constrained Utility Accrual (or RUA) scheduling algorithm [wrjb04] and (2) the Dependent Activity Scheduling Algorithm (or DASA) [cla90]. We develop wait-free versions of RUA and DASA using the space-optimal protocol in [crj05].

We analytically compare RUA's and DASA's wait-free and lock-based versions. We establish upper bounds on the maximum increase in utility that is possible with wait-free over lock-based. The upper bounds --- the first such --- verify our hypothesis. Our measurements from a POSIX RTOS implementation reveal that during under-loads, wait-free algorithms yield optimal utility for step TUFs and significantly higher utility (than lock-based) for non-step TUFs.

Thus, the work's central contribution is wait-free UA scheduling algorithms with the upper bounds on their maximum possible increase in activity utility over lock-based for the minimum additional space cost, and the resulting tradeoff. We are not aware of any other wait-free UA algorithm.

- Synchronization in RUA

RUA [wrjb04] considers activities subject to arbitrarily shaped TUF time constraints and concurrent sharing of non-CPU resources including logical (e.g., data objects) and physical (e.g., disks) resources. The algorithm allows concurrent resource sharing under mutual exclusion constraints. RUA's objective is to maximize the total utility accrued by all activities. To develop RUA's wait-free version, we first overview the original lock-based algorithm.

- Lock-Based RUA

RUA's scheduling events include task arrivals, task departures, and lock and unlock requests. When RUA is invoked, it first builds each task's dependency list---that arises due to mutually exclusive object sharing---by following the chain of object request and ownership. The algorithm then checks for deadlocks by detecting the presence of a cycle in the object/resource graph --- a necessary condition for deadlocks. Deadlocks are resolved by aborting that task in the cycle which will likely contribute the least utility.

After handling deadlocks, RUA examines tasks in the order of non-increasing potential utility densities (or PUDs). The PUD of a task is the ratio of the expected task utility to the remaining task execution time, and thus measures the task's return of investment. The algorithm inserts a task and its dependents into a tentative schedule, in the order of their critical times, earliest critical time first. Critical time is the time at which the task TUF has zero utility--i.e., the ``deadline" time (all TUFs are assumed to have such a time). The insertion is done by respecting the tasks' dependencies. After insertion, RUA checks the schedule's feasibility. If infeasible, the inserted task and its dependents are rejected. The algorithm repeats the process until all tasks are examined, and selects the task at the schedule head for execution. If a task's critical time is

reached and its execution has not been completed, an exception is raised, which is also a scheduling event, and the task is immediately aborted.

In [wrjb04], Wu *et al.* bound the maximum blocking time that a task may experience under RUA for the special-case of the single-unit resource model.

Theorem 1 (RUA's Blocking Time) Under RUA with the single-unit resource model, a task T_i can be blocked for at most the duration of *min(n,m)* critical sections, where n is the number of tasks that can block T_i and have longer critical times than T_i, and m is the number of resources that can be used to block T_i.
Proof. See [wrjb04].

- Wait-Free RUA

We focus on the single-unit resource model for developing RUA's wait-free version. With wait-free synchronization, RUA is significantly simplified. Scheduling events now include only task arrivals and task departures --- lock and unlock requests are not needed anymore. Further, no dependency list arises and need to be built. Moreover, deadlocks will not occur due to the absence of object/resource dependencies. All these reduce the algorithm's complexity. RUA's wait-free version is described in Figure 2.2-2.

> **Input** : T_r, task set in the ready queue
> **Output** : selected thread T_{exe}
> Initialization: t=t$_{cur}$, σ=NULL
> **For** all $T_i \in T_r$
>   **If** feasible(T_i)
> T_i.PUD=U$_i$(t+T_i.ExecTime) / T_i.ExecTime;
>   **else**
>   abort(T_i);
> σ $_{tmp1}$ = sortByPUD(T_r);
> **For** all $T_i \in$ σ $_{tmp1}$ from head to tail
>   **If** T_i.PUD>0
>   σ $_{tmp2}$= σ;
>   InsertByDeadline(T_i, σ $_{tmp2}$);
>   If feasible(σ $_{tmp2}$)
>   σ = σ $_{tmp2}$;
>   **else**
>   break;
> T$_{exe}$=headOf(σ);
> **return** T$_{exe}$;

Figure 2.2-2 Wait-free RUA.

Lock-based RUA's time complexity grows as a function of the number of tasks, while that for wait-free RUA, it grows as a function of the number of readers. (The cost of lock-based RUA is independent of the number of objects, as the dependency list built by RUA may contain all tasks in the worst-case, irrespective of the number of objects.) Because the number of readers cannot exceed the number of tasks, the number of readers can be replaced with the number of tasks.

With n tasks and m readers, the time complexity of lock-based RUA is $O(n^2 logn)$ [wrjb04], while that of wait-free RUA is $O(n^2+m)$, as Figure 2.2-2 shows. As the number of readers m, is bounded by n, wait-free RUA improves upon lock-based RUA from $O(n^2 logn)$ to $O(n^2)$.

44

We now formally compare task sojourn times under wait-free and lock-based versions of RUA. We assume that all accesses to lock-based shared objects require r units of time, and that to wait-free shared objects require w units. The computation time c_i of a task T_i can be written as $c_i=u_i+m_i \times t_{acc}$, where u_i is the computation time excluding accesses to shared objects; m_i is the number of shared object accesses by T_i; and t_{acc} is the maximum computation time for any object access---i.e., r for lock-based objects and w for wait-free objects.

Theorem 2 (Comparison of RUA's Sojourn Times) Under RUA, as the critical section t_{acc} of a task T_i becomes longer, the difference between the sojourn time with lock-based synchronization, s_{lb}, and that with wait-free protocol, s_{wf}, converges to the range:
$$0 \le s_{lb} - s_{wf} \le r \times min(n_i, m_i),$$
where n_i is the number of tasks that can block T_i and have longer critical times than T_i, and m_i is the number of shared data objects that can be used to block T_i.

Proof.
The sojourn time of a task T_i under RUA with lock-based synchronization includes the execution time $c_i=u_i+m_i \times r$, the preemption time I_i, and the blocking time B_i. Based on Theorem 1, the blocking time B_i is at most $r \times min(n_i, m_i)$. On the other hand, the sojourn time of task T_i under RUA with wait-free protocol does not include any blocking time. Therefore, the difference between lock-based synchronization and wait-free is at most $m_i \times (r-w) + r \times min(m_i, n_i)$. Assuming that the data for synchronization is large enough such that the execution time difference in the algorithm between lock-based synchronization and wait-free becomes negligible (i.e., the time for reading and writing the data object becomes dominant in the time for synchronization), then r and w converge and become equal. In this case, the sojourn time of T_i under lock-based synchronization is longer than that under wait-free by $r \times min(m_i, n_i)$.

The reduced sojourn time of a task under wait-free increases the accrued utility of the task, for non-increasing TUFs. Further, this potentially allows greater number of tasks to be scheduled and completed before their critical times, yielding more total accrued utility (for such TUFs).

Based on Theorem 2, we can now estimate the difference in the Accrual Utility Ratio (or AUR) between wait-free and lock-based, for non-increasing TUFs. AUR is the ratio of the actual accrued utility to the maximum possible utility.

Corollary 1 Under RUA, with non-increasing TUFs, as the critical section t_{acc} of a task T_i becomes longer, the difference in AUR, $\Delta AUR = AUR_{wf} - AUR_{lb}$, between lock-based synchronization and wait-free converges to:
$$0 \le \Delta AUR \le \sum_{i=1}^{N} \frac{U_i(s_{wf}) - U_i(s_{wf} + r \cdot min(m_i, n_i))}{U_i(0)}$$
where $U_i(t)$ denotes the utility accrued by task T_i when it completes at time t, and N is the number of tasks.

Proof.
It follows directly from Theorem 2.

When the data for synchronization is small and the time for reading and writing the shared data object is not dominant, r and w are more dependent on the object sharing algorithm. The execution time of lock-based synchronization, r, includes the time for the locking and unlocking procedure (needed for mutual exclusion), executing the scheduler, and accessing the shared object, while w includes the time for controlling the wait-free protocol's variables and accessing the shared object. The wait-free protocol does not activate the scheduler, and hence avoids significant system overhead. Consequently, w's of many wait-free protocols are known to be

shorter than r [crj05,hps02]. Thus, no matter what the size of the data to communicate between tasks is, wait-free synchronization conclusively accrues more utility compared with lock-based synchronization.

- Synchronization in DASA

DASA [cla90] considers activities subject to step-shaped TUFs and concurrent sharing of non-CPU resources (e.g., data objects, disks) under mutual exclusion constraints and under the single-unit resource request model. Thus, DASA's model is a proper subset of RUA: DASA is restricted to step TUFs and the single-unit model, while RUA allows arbitrarily shaped TUFs and the multi-unit model (we focus on RUA's single-unit model here).

Like RUA, DASA's objective is to maximize the total utility accrued by all activities. DASA's basic operation is identical to that of RUA for the single-unit model (see Section (4)). Thus, for the single-unit model, RUA's behavior subsumes DASA's. Therefore, in [wrjb04], Wu et al. also show that the maximum blocking time that a task may suffer under DASA is identical to that under RUA (for the single-unit model), which is stated in Theorem 1.

- Wait-Free DASA

Since TUFs under DASA are step-shaped, shorter sojourn time does not increase accrued utility, as tasks accrue the same utility irrespective of when they complete before their critical times, as long as they do so. However, shorter sojourn time is still beneficial, as it reduces the likelihood of missing task critical times. Hence, lesser the number of tasks missing their critical times, higher will be the total accrued utility.

Wait-free synchronization prevents DASA from loosing utility no matter how many dependencies arise. Similar to wait-free RUA, wait-free DASA is also simplified: Scheduling events now include only arrivals and departures, no dependency list needs to be built, and no deadlocks will occur.

The time complexities of lock-based and wait-free DASA are identical to that of lock-based and wait-free RUA: $O(n^2)$ [cla90] and $O(n^2+m)$, respectively. Similar to wait-free RUA, as m is bounded by n, wait-free DASA improves upon lock-based DASA from $O(n^2 log n)$ to $O(n^2)$. The comparison of DASA's sojourn times under lock-based and that under wait-free is similar to Theorem 2.

Theorem 3 (Comparison of DASA's Sojourn Times) Under DASA, as the critical section t_{acc} of a task T_i becomes longer, the difference between the sojourn time with lock-based synchronization, s_{lb}, and that with wait-free protocol, s_{wf}, converges to:
$0 \leq s_{lb} - s_{wf} \leq r \times min(n_i, m_i)$,
where n_i is the number of tasks that can block T_i and have longer critical times than T_i, and m_i is the number of shared data objects that can be used to block T_i.
Proof.
See proof of Theorem 2.

- Implementation Experience

We implemented the lock-based and wait-free algorithms in the *meta-scheduler* scheduling framework [lrsf04], which allows middleware-level real-time scheduling atop POSIX RTOSes. We used QNX Neutrino 6.3 RTOS running on a 500 MHz Pentium-III processor in our implementation.

Our task model for computing the wait-free buffer size follows the model in [hps02]. We determine the maximum number of times the writer can interfere with the reader, N^{max} as:

$$N^{max} = \max(2, \left\lceil \frac{P_R - (C - C_R)}{P_W} \right\rceil)$$

P_R and P_W denote the reader's and the writer's period, respectively. For simplicity, we set the task critical times to be the same as the task periods. C is the reader's worst-case execution time, and C_R is the time needed to perform a read operation.

Table 2.2-1 shows our task parameters. We consider a task set of 10 tasks, which includes 5 readers and 5 writers, mutually exclusively sharing at most 5 data objects. We set C_R for each object to be approximately 20 % of C for each reader, which implies that tasks share large amounts of data. We allow a reader to read from 1 object to at most 5 objects. We also vary the number of readers from 1 to 5. The minimum buffer size needed for the wait-free protocol is calculated by [crj05]. The actual amount of memory needed is the buffer size multiplied by the message size in bytes.

For each experiment, we generate approximately 16,000 tasks and measure the AUR and the CMR (or critical time meet ratio) under RUA's and DASA's lock-based and wait-free versions, where CMR is the ratio of the number of tasks that meet their critical times to the total number of task releases. The performance comparison between both are shown with the varying number of shared objects and the varying number of tasks.

Table 2.2-1 Experimental Parameters for Tasks

Name	P(msec)	C(msec)	Shared Objects
Writer1	100	10	r_1
Writer2	100	10	r_2
Writer3	100	10	r_3
Writer4	100	10	r_4
Writer5	100	10	r_5
Reader1	900	100	$r_1\ r_2\ r_3\ r_4\ r_5$
Reader2	1000	100	$r_5\ r_1\ r_2\ r_3\ r_4$
Reader3	1100	100	$r_4\ r_5\ r_1\ r_2\ r_3$
Reader4	1200	100	$r_3\ r_4\ r_5\ r_1\ r_2$
Reader5	1300	100	$r_2\ r_3\ r_4\ r_5\ r_1$

For each experiment, we generate approximately 16,000 tasks and measure the AUR and the CMR (or critical time meet ratio) under RUA's and DASA's lock-based and wait-free versions, where CMR is the ratio of the number of tasks that meet their critical times to the total number of task releases. The performance comparison between both are shown with the varying number of shared objects and the varying number of tasks.
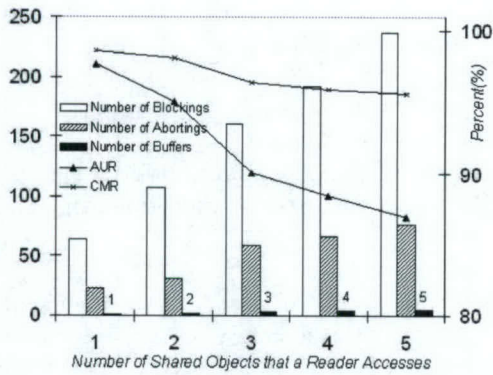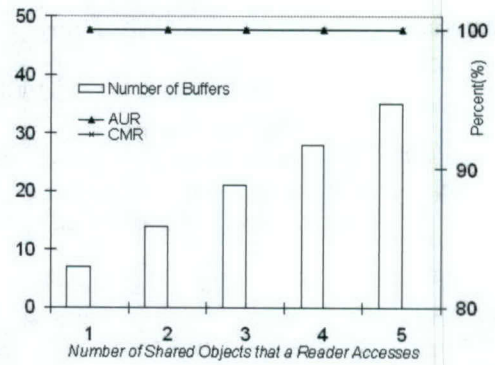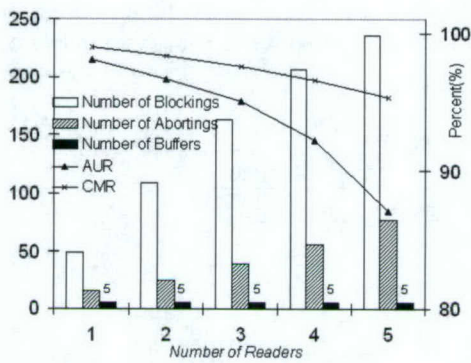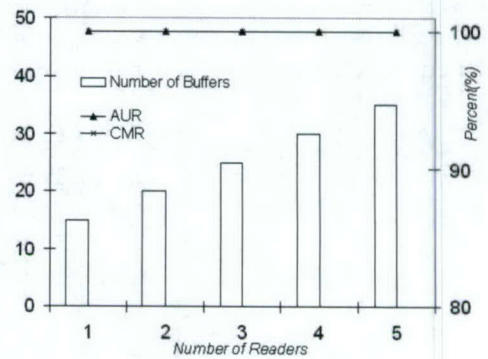
(a) Lock-based   (b) Wait-free

Figure 2.2-3 Performance of lock-based and wait-free DASA under increasing number of shared objects.
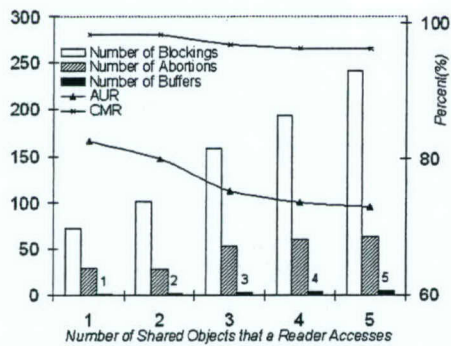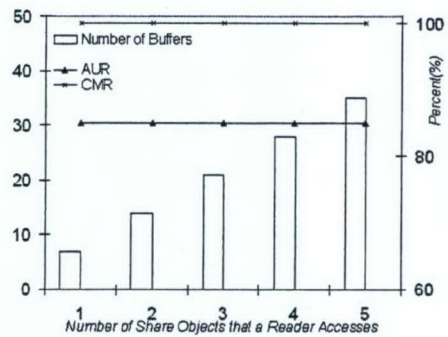

(a) Lock-based   (b) Wait-free

Figure 2.2-4 Performance of lock-based and wait-free DASA under increasing number of readers.

Figure 2.2-3 and Figure 2.2-4 show lock-based and wait-free DASA's AUR and CMR (on the right-side y-axes), under increasing number of shared data objects and under increasing number of reader tasks, respectively. The figures also show (on the left-side y-axes) the number of buffers used by lock-based and wait-free, as well as the number of task blockings' and task abortions that occur under lock-based.
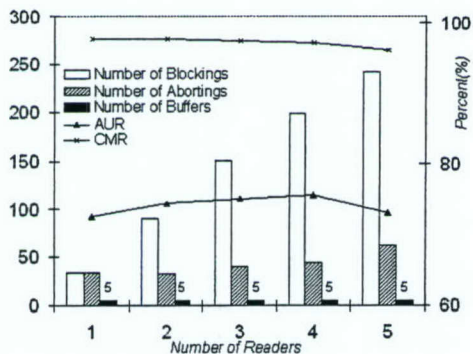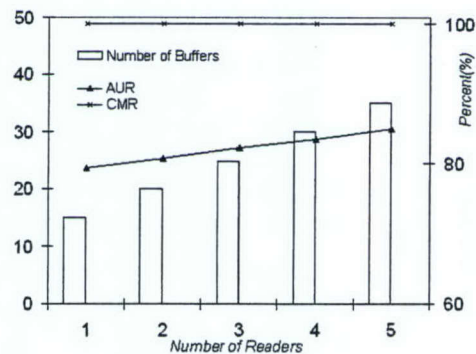
(a) Lock-based   (b) Wait-free

Figure 2.2-5 Performance of lock-based and wait-free RUA under increasing number of shared objects.

(a) Lock-based   (b) Wait-free

Figure 2.2-6 Performance of lock-based and wait-free RUA under increasing number of readers.

From Figures 2.2-3(a) and 2.2-4(a), we observe that the AUR and CMR of lock-based DASA decrease as the number of shared objects and number of readers increase. This is because, as the number of shared objects and readers increase, a greater number of task blockings' occurs, resulting in increased sojourn times, critical time-misses, and consequent abortions.

Wait-free DASA is not subject to this behavior, as Figures 2.2-3(b) and 2.2-4(b) show. Wait-free DASA achieves 100 % AUR and CMR even as the number of shared objects and readers increase. This is because, wait-free eliminates task blockings'. Consequently, the algorithm produces a critical time (or deadline)-ordered schedule, which is optimal for under-load situations (i.e., all critical times are satisfied). Thus, all tasks complete before their critical times, and the algorithm achieves the maximum possible total utility.

However, the number of buffers needed for wait-free increases as the number of objects and readers increase. But Algorithm in [crj05] is space-optimal --- the needed buffer size is the absolute minimum possible.

Similar to the DASA experiments, we compare the performance of RUA's lock-based and wait-free versions. Since RUA allows arbitrarily-shaped TUFs, we consider a heterogenous class of TUF shapes including step, parabolic, and linearly-decreasing. The results are shown in Figures

49

2.2-5 and 2.2-6. We observe similar trends as that of DASA's: Lock-based RUA's AUR and CMR decrease as the objects and readers increase, due to increased task blockings'.

Similar to DASA, wait-free sharing alleviates task blockings' under RUA. Consequently, RUA produces optimal-schedules during under-load situations in terms of meeting all task critical times, and thus yields 100% CMR.

RUA with wait-free sharing yields greater AUR than that under lock-based, as objects and readers increase. However, unlike DASA, RUA does not yield 100% AUR with wait-free, because tasks accrue different utility depending upon when they complete, even when they do so before task critical times (due to non-step shapes). Further, the algorithm does not necessarily complete tasks at their optimal times as that scheduling problem is NP-hard (and RUA is a heuristic).

2.2.3 Importance/Relevance

We believe that the TUF/UA real-time technology developed in this task is directly relevant to DoD's network-centric warfare concept, Navy combatant systems including DD(x), and other DoD systems such as Air Force's next generation command and control aircrafts. In fact, the fundamental aspects of this class of real-time problems include:

1. Need for transparent programming and scheduling abstractions for distributed computation workflows that are subject to time constraints

2. Systems that are subject to significant run-time uncertainties that are often manifested in execution and communication times, and event and failure occurrences that are non-deterministically distributed

3. Systems that are subject to transient and permanent overloads

4. Need for time-critical and mission-oriented resource management (i.e., timely management of resources in the best interest of the current application mission)

5. Need for industry/commercial standards- and COTS-based solutions for portability, robustness, and maintainability.

All these aspects are directly addressed by Task 2.2 research. In particular, Real-Time CORBA 1.2's and DRTSJ's distributable threads abstraction provides a transparent programming and scheduling abstraction for distributed real-time computation workflows. Further, the class of TUF/UA scheduling algorithms, TMAR protocols, synchronization mechanisms, and policy-based network QoS management schemes target application activities, whose execution/communication latencies and event/failure occurrences are non-deterministically distributed and are subject to overloads. TUF/UA algorithms provide time-critical and mission-oriented resource management by (system-wide) scheduling to maximize system-wide accrued utility, where utility is mapped to application-level QoS. Consequently, utility maximization leads to managing system resources to maximize utility achieved for the users by the system. Furthermore, Task 2.2's work on the DRTSJ industry standard directly promotes industry/commercial standards and COTS-based solutions.

DD(X) is currently using RTSJ, and is building a distributed real-time infrastructure using RTSJ. The DD(X) team has expressed significant interest in using DRTSJ – in particular, the distributable threads abstraction and end-to-end timing analysis capability. We believe that DD(X) can directly leverage DRTSJ's advanced adaptive time-critical (TUF/UA) resource

management techniques, and DRTSJ's synergy with RTSJ. Thus, Task 2.2 research is directly relevant to Navy systems and other DoD systems.

2.2.4 Productivity

Journal publications

1. H. Wu, B. Ravindran, E. D. Jensen, "Utility Accrual, Real-Time Scheduling Under the Unimodal Arbitrary Arrival Model with Energy Bounds," *ACM Transactions on Embedded Computing Systems*, Submitted February 2005 (under review)

2. H. Wu, B. Ravindran, E. D. Jensen, and P. Li, "Time/Utility Function Decomposition Techniques for Utility Accrual Scheduling Algorithms in Real-Time Distributed Systems," *IEEE Transactions on Computers*, Accepted March 2005

3. H. Wu, B. Ravindran, E. D. Jensen, and P. Li, "Energy-Efficient, Utility Accrual Scheduling under Resource Constraints for Mobile Embedded Systems," *ACM Transactions on Embedded Computing Systems*, Accepted with minor revisions, February 2005

Conference publications

1. H. Cho, B. Ravindran, and E. D. Jensen, "On Utility Accrual Processor Scheduling with Wait-Free Synchronization for Embedded Real-Time Software," *2005 IEEE/ACM/ IFIP CODES+ISSS*, Submitted April 2005 (under review)

2. H. Cho, B. Ravindran, and E. D. Jensen, "On Lock-Free Synchronization for Dynamic Embedded Real-Time Software," *ACM EMSOFT 2005*, Submitted April 2005 (under review)

3. H. Wu, U. Balli, B. Ravindran, and E. D. Jensen, "'Utility Accrual Real-Time Scheduling under Variable Cost functions," *2005 IEEE RTCSA*, Submitted April 2005 (under review)

4. H. Cho, B. Ravindran, and E. D. Jensen, "A Space-Optimal, Wait-Free Real-Time Synchronization Protocol," *2005 IEEE Euromicro Conference on Real-Time Systems (ECRTS 05)*, Accepted March 2005

5. B. Ravindran, E. D. Jensen, and P. Li, "On Recent Advances in Time/Utility Function Real-Time Scheduling and Resource Management," *2005 IEEE International Symposium on Object-oriented Real-time distributed Computing (ISORC)*, Accepted February 2005

6. P. Li, H. Cho, B. Ravindran, and E. D. Jensen, "Stochastic, Utility Accrual Real-Time Scheduling with Task-Level and System-Level Timeliness Assurances," *2005 IEEE International Symposium on Object oriented Real-time distributed Computing (ISORC)*, Accepted February 2005

7. H. Wu, B. Ravindran, and E. D. Jensen, "Energy-Efficient, Utility Accrual Real-Time Scheduling Under the Unimodal Arbitrary Arrival Model," *ACM Design, Automation, and Test in Europe (DATE)*, March, 2005

8. S. Feizabadi, B. Ravindran, and E. D. Jensen, "MSA: A Memory-Aware Utility Accrual Scheduling Algorithm," *ACM Symposium On Applied Computing (Track on Embedded Systems)*, March 2005

Students supported
Jonathan Anderson, Jan. 15, 2005 – present
Hyeonjoong Cho, Jan. 15, 2005 – present

2.2.5 References

[cla90]   R. K. Clark, "Scheduling Dependent Real-Time Activities," PhD thesis, CMU CS Dept., 1990

[cjk+99]   R. K. Clark, E. D. Jensen, et al., "An adaptive, distributed airborne tracking system," In *IEEE WPDRTS*, pages 353--362, April 1999

[hor74]   W. Horn, "Some Simple Scheduling Algorithms," *Naval Research Logistics Quarterly*, 21:177--185, 1974.

[jlt85]   E. D. Jensen, C. D. Locke, and H. Tokuda, "A time-driven scheduling model for real-time systems," In *IEEE RTSS*, pages 112--122, December 1985

[loc86]   C. D. Locke, "Best-Effort Decision Making for Real-Time Scheduling," PhD thesis, Carnegie Mellon University, 1986

[wrjb04]   H. Wu, B. Ravindran, E. D. Jensen, and U. Balli, "Utility Accrual Scheduling Under Arbitrary Time/Utility Functions and Multiunit Resource Constraints," *IEEE Real-Time Computing Systems and Applications*, April 2004

[srl90]   L. Sha, R. Rajkumar, and J P. Lehoczky, "Priority inheritance protocols: An approach to real-time synchronization," *IEEE Trans. Computers*, 39(9):1175--1185, 1990

[kr93]   H. Kopetz and J. Reisinger, "The non-blocking write protocol NBW", *IEEE RTSS*, 131--137, 1993

[cb97]   J. Chen and A. Burns, "A fully asynchronous reader/writer mechanism for multiprocessor real-time systems," *Technical Report YCS-288*, CS Dept., University of York, May 1997.

[hps02]   H. Huang, P. Pillai, and K. G. Shin, "Improving wait-free algorithms for interprocess communication in embedded real-time systems," *USENIX Annual Technical Conference*, pages 303--316, 2002

[arj97]   J. H. Anderson, S.~Ramamurthy, and K. Jeffay, "Real-time computing with lock-free shared objects," *ACM TOCS*, 15(2):134--165, 1997

[crj05]   H. Cho, B. Ravindran, and E. D. Jensen, "A space-optimal, wait-free real-time synchronization protocol," *IEEE ECRTS*, 2005.

2.3 Task 2.3 Network Interoperability and Quality of Service

2.3.1 Overview

Task Goal: The goal of Task 2.3 is to integrate network services (as investigated in Task 2.1) with real-time middleware (as investigated in Task 2.2). Specifically, we will investigate and develop methods and mechanisms to integrate policy-based quality of service (QoS) capabilities at the network level, and perhaps at the link layer, with real-time services offered by middleware.

Organization: This task is managed by Scott Midkiff using the following personnel:
Scott F. Midkiff, task director
Luiz A. DaSilva, faculty
Binoy Ravindran, faculty

Summary: Task 2.3 integrates results from Tasks 2.1 and 2.2. As these tasks are just beginning, no significant activity that has taken place for Task 2.3 during the reporting period. Thus, the following sections summarize subtasks and schedule.

2.3.2 Task Activities for the Period

Task Objective: The goal of Task 2.3 is to integrate network services (from Task 2.1) with real-time middleware (from Task 2.2).

Accomplishments during reporting period: Minimal activities pertaining to this subtask took place during the reporting period.

Links to other tasks: This task integrates results from Task 2.1 and Task 2.2. It is also potentially synergistic with Task 2.4 (Cross-Layer Optimization) as it may be possible to integrate optimizations at the link and network layer with requirements presented by the real-time middleware.

Schedule: The schedule for this task is as follows.
– Plan integration approach (April-June 2005)
– Begin integration based on preliminary results (July-December 2005)
– Integrate cross-layer design features (October-December 2005)
– Integrate protocols using test bed (January-March 2006)
– Refine protocols based on performance evaluation and demonstrations (April-June 2006)

Personnel: No personnel were assigned to this subtask for the reporting period.

2.3.3 Importance/Relevance

Many military systems rely on real-time operation, but can often be characterized using "soft" real-time constraints. This work paves the way to providing real-time capabilities, based on time-utility functions (TUFs), in an ad hoc network environment.

We presented this task to personnel from the Office of Naval Research and the Naval Research Laboratory (NRL) as part of the AWINN kickoff meeting on March 31, 2005 in Blacksburg, VA.

2.3.4 Productivity

There is currently nothing to report for Task 2.3.

2.4 Task 2.4 Cross-Layer Optimization

2.4.1 Overview

Task Goal: The goal of this task is to investigate and develop methods and metrics to characterize and evaluate the interaction between physical, data link, network and application layer protocols.

Organization: This task is managed by Dr. R. Michael Buehrer and Dr. Scott Midkiff.

Dr. R. Michael Buehrer, faculty
Dr. Scott Midkiff, faculty
Dr. Tom Hou, faculty
Qiao Chen, GRA
Swaroop Venkatesh, GRA

Summary: This quarter we focused on two subtasks: (a) Cross-layer design for UWB position-location networks and (b) collaborative radio networks.

2.4.2 Task Activities for the Period

Subtask 2.4.1a Cross-Layer Design for Ultra-Wideband Position-Location Networks

Ultra-Wideband (UWB) signals have been used in the military for radar applications since the 1970s. In February 2002 the FCC legalized the use of UWB by releasing a set of spectral masks that stipulated the emission level and frequency of operation for imaging, radar, and communication purposes, sparking a flurry of activity in UWB technology. Impulse Radio is a form of UWB signaling which uses streams of baseband pulses of very short duration, typically on the order of a nanosecond, thereby spreading the power spectral density of the radio signal from near D.C. to a few gigahertz. Since UWB systems have to operate in the highly populated frequency range below a few gigahertz, impulse radios must not only contend with a variety of interfering signals, but must also ensure that they do not interfere with existing narrowband radio systems by satisfying the restrictions on power spectral density imposed by the FCC. These constraints on the power spectral density necessitate the use of spread-spectrum techniques. A simple means for spreading the spectrum of these ultra-wide bandwidth low-duty cycle pulse trains is time-hopping, with data modulation accomplished by additional pulse position modulation at the rate of many pulses per data symbol. One of the most important advantages of impulse-based UWB is its resistance to multipath fading. Multipath resolution down to a nanosecond in differential path delay leads to an elimination of significant multipath fading. This may considerably reduce fading margins in link budgets and may allow low transmission power operation.

Impulse radio has properties that make it a viable candidate for use in ad hoc networks of nodes where nodes exchange data, location and sensing information at high data rates. The fine time resolution of UWB pulses can be used to extract extremely accurate range information. Therefore, UWB signals can be used to simultaneously communicate data as well as distance information, making them ideal for position-location networks. This is discussed in detail in the next section.

In outdoor environments, accurate, reliable position information can be obtained via GPS. However, there are many situations where GPS is either impractical or impossible. Specifically,

55

indoor scenarios or situations where GPS receivers are too bulky or expensive require other solutions. One example is the command and control of a firefighter operation where personnel are deployed into a building. For safety and efficiency purposes, it would be extremely helpful for a command center outside the building to be established for not only communication but also for position tracking. In such a case we require an ad hoc position location network that is independent of GPS and is not reliant on pre-existing infrastructure.

Traditional ranging (and position location) applications have relied on optical (laser), ultrasound, or narrowband RF physical layers. However, we propose the use of UWB because of its usefulness in harsh environments and its covertness for tactical applications. It is well known that optical and ultra-sound have limited range in harsh environments (e.g., harsh multipath or severe weather) and may fail completely when the line-of-sight is blocked. Additionally, narrowband RF solutions have difficulty in dense multipath due to severe multipath fading. UWB, on the other hand has strong material penetration capabilities (specifically in the lower bands approved by the FCC for radar applications) as well as multipath fading resistance. The narrow pulse duration of UWB signals also provide the opportunity for extremely (order of centimeters) good accuracy. Additionally, UWB provides other potential advantages such as jamming resistance and low probability of detection.

Position-Location networks can be designed to meet the requirements specific to different applications. For the application of fire-fighter location networks, for instance, the position-location network starts with a small number of anchors located outside the area of interest whose positions are known *a priori* (perhaps via GPS or a relative local co-ordinate system). A controller is also located near the anchors for command and control and possibly to assist in global position determination (note however we are focused here on distributed algorithms as opposed to centralized solutions). A large number of nodes are deployed into a region of interest (deployment options not considered here but could be either manually as in a fire-fighter scenario, via tiny robots, dispersed via UAV, or could be launched into the area of interest). The network has two distinct phases. First, the deployed nodes must learn their position based on limited connectivity and with only a few nodes being able to range to the anchors. After the deployed nodes have established their own positions, the second phase of the network involves assisting any mobile node that enters the area. The mobile nodes use the deployed nodes as virtual anchors to determine their locations. Additionally, the deployed nodes provide a multi-hop communication network to relay position information back to command-and-control. These nodes must also update their position information at a rate that depends on the stability of the environment, the node speed, and whether the node is being used for other purposes.

The described network has several advantages in terms of versatility, but because of the UWB physical layer there are obviously several research issues that need to be solved to maximize the potential of such a network. The issues arise from the use of the UWB physical layer, the lack of fixed infrastructure and the fact that the network has an unknown size *a priori*. Specifically, at the physical layer, accurate acquisition techniques are required for ranging and consequently accurate position location determination. Additionally, due to the potential for dense multipath and the lack of a line-of-sight component, the position estimation routine must be able to ascertain the reliability of the individual range estimates. At the data link layer, we must determine a medium access control technique that is specifically designed for position location, and this is the subject of the next section.

For the application of position location, we observe that the desired network is a unique hybrid of mobile ad hoc and sensor networks. Specifically, the data sinks of the network are mainly the mobile and control nodes and the physical quantity being measured by the remaining stationary

sensor nodes is the physical location of the mobile nodes. The size of the network grows with time over the area of coverage and therefore automated node discovery and routing are essential. Since the size of the network grows with time, we require the MAC protocol to be scalable. The MAC protocol for this network needs to provide node discovery, fair and reliable multi-hop data transfer between nodes and be able to adapt to the mobility of nodes and to node failure. We also require fairly up-to-date knowledge of the location of the mobile nodes, and therefore we also need to ensure that latency requirements are met. There is a trade-off between update-rate and reliability, and therefore our MAC protocol should allow us to trade one quantity for another. Since the nodes in the ad hoc network case are designed to be battery-powered, once again the MAC protocol needs to be power-efficient.

Another unique feature of the network is the impulse-based UWB physical layer. Due to power constraints on UWB impulse radio, in order for impulse radios to achieve significant transmission ranges we would have to use several pulses per bit and therefore reduce the data rates of these networks. This low data rate over a wide transmission bandwidth automatically implies large spreading gains, and therefore we envision Time-Hopped (TH) or Direct Sequence (DS) spreading to be an integral feature of the UWB signals used.

We have proposed a MAC protocol based on the Common-Transmitter Spread-Spectrum Multiple-Access protocol (CT-SSMA). CT-SSMA is essentially a spreading-code-assignment approach to establishing communication between exactly two nodes within a packet radio network. In our case, given a certain node in the network, the number of nodes around it that are capable of ranging to this node is not known beforehand and can change with time. Therefore, we adapt the CT-SSMA protocol to enable an arbitrary number of users to communicate with the node that contends for the common code. The performance of this protocol has been compared with CSMA in terms of the location error and a sample result is shown in Figure 2.4-1. We see that the location error in the case of the proposed approach is significantly smaller than with CSMA.
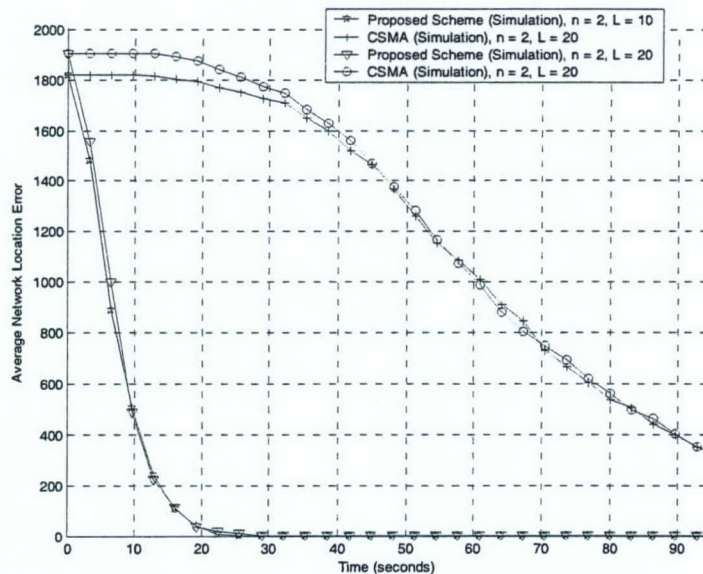

Figure 2.4-2 Comparison of the proposed MAC protocol with CSMA in terms of the location error convergence with time.

Several issues regarding the design of MAC protocols need to be investigated. For example, how does one characterize an optimal MAC protocol for position-location errors? What metric determines the performance of a MAC protocol for these networks? It seems intuitive that there should be a strong link between the throughput of the MAC protocol used and the rate of convergence of location error, but this result needs to be proved formally. The performance of the proposed MAC protocol can be enhanced with the use of power-control schemes. Power control schemes based on location estimates can be derived and UWB position-location networks seem ideally suited to cross layer design techniques.

The above described UWB position-location networks appear to be well suited to cross-layer design techniques. The following possibilities are evident:

1. The position-location estimates obtained at the application layer can be used for routing in the network layer.

2. The same estimates can also be used to implement power-control schemes in the MAC layer to make MAC protocols power-efficient.

3. These estimates and other parameters can be used to modify physical layer parameters to maximize efficiency and improve performance.

4. It is possible to use connectivity information to aid the solution of the location estimation problem in certain situations.

Therefore, the avenues for cross-layer design research for UWB position-location networks seem to be numerous and fairly diverse.

Subtask 2.4.1b Cross-Layer Design of Cooperative UWB Networks

Sub-Task objective: MIMO systems benefit from beam-forming gains, diversity gains and spatial multiplexing. By allowing cooperation between mobile terminals, cooperative relaying actually builds a virtual MIMO system. This idea has spurred a great deal of recent research. However, most of this research effort has been limited to narrow band communication systems. The work in this sub-task extends these concepts to wide band systems, and seeks to develop cross-layer design principles for such networks.

Accomplishments during reporting period: There are three cooperative signaling methods identified in the research literature: amplify and forward (retransmit), detect and forward, and coded cooperation. In the amplify and forward method, the relay node transmits a noisy (received) version of the signal of its partner to the same receiver as illustrated in Figure 2.4-2. This method is simple and straight forward, but it is not a trivial thing at the relay node to sample, amplify, and retransmit the analogy signal. The second technique, detect and forward, the relay detects the source's bits and retransmits them, and the relay node only works in cooperative mode if the instantaneous SNR is high. The downside of this technique arises when unsuccessful detection occurs at the relay node. Finally, the last technique, coded cooperation, integrates cooperation with channel coding, providing the best performance among the three.

In the research stage of cooperative UWB networks, we explore detect-and-forward methods, and expand it to the multiple relay case, assuming that the relay nodes can detect transmitter's signal without error. Also, the transmit signals and the relay signals are assumed to arrive at the receiver symbol (but not pulse) synchronous. Figure 2.4-2 shows the basic structure of the cooperative UWB communication system with one relay nodes.
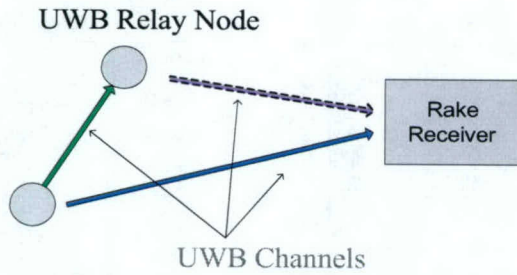
UWB Relay Node

Rake Receiver

UWB Channels

Figure 2.4-2 Cooperative UWB communication systems.

For a SISO (impulse based) UWB system, the transmitted signal has the form:

$$s(t) = \sqrt{E_p} \sum_{i=-\infty}^{\infty} b_i \sum_{n=0}^{N_x-1} w(t - nT_w - iT_f) \tag{2.4-1}$$

where $b_i = \pm 1$ are the data bits, $w(t)$ is the unit-energy transmit pulse with a length of T_w, N_x is the length of signal sequence, and T_f is the symbol duration which is large enough to avoid ISI. Assuming an L-path tap-delay channel model, the UWB channel is represented as:

$$h(t) = \sum_{l=1}^{L} \alpha_l \delta(t - \tau_l) \tag{2.4-2}$$

where α_l and τ_l are the amplitude and delay of the lth multipath component, respectively. The received signal, in the time interval $\lfloor kT_f \quad (k+1)T_f \rfloor$, can be written as:

$$r(t) = \sqrt{E_p} b_k \sum_{l=1}^{L} \alpha_l \sum_{n=0}^{N_x-1} w(t - nT_w - \tau_l) + n(t) \tag{2.4-3}$$

where k is a positive integer, and $n(t)$ is zero-mean additive white Gaussian noise with power spectral density $\frac{N_0}{2}$. Intuitively, we can rewrite the $r(t)$ as:

$$R = \sqrt{E_p} S * H + N \tag{2.4-4}$$

where S, H, N is unit-energy transmit signal, channel impulse response and AWGN noise, '$*$' denotes convolution operations. Adding one relay node, received signal has the following form:

$$R = \sqrt{\frac{E_p}{2}} S * H_1 + \sqrt{\frac{E_p}{2}} S * H_2 + N \tag{2.4-5}$$

In Figure 2.4-3a and 2.4-3b, two UWB channels are randomly chosen from a measurement database, the SISO performance is plotted with blue curves and red curves provide the performance of cooperative transmission. Comparing these two plots, it is obvious that no diversity gain is guaranteed when adding relay nodes. This is due to the fact that the channel impulse responses H_1 and H_2 are not naturally coherently combined, resulting in destructive interference in some cases..
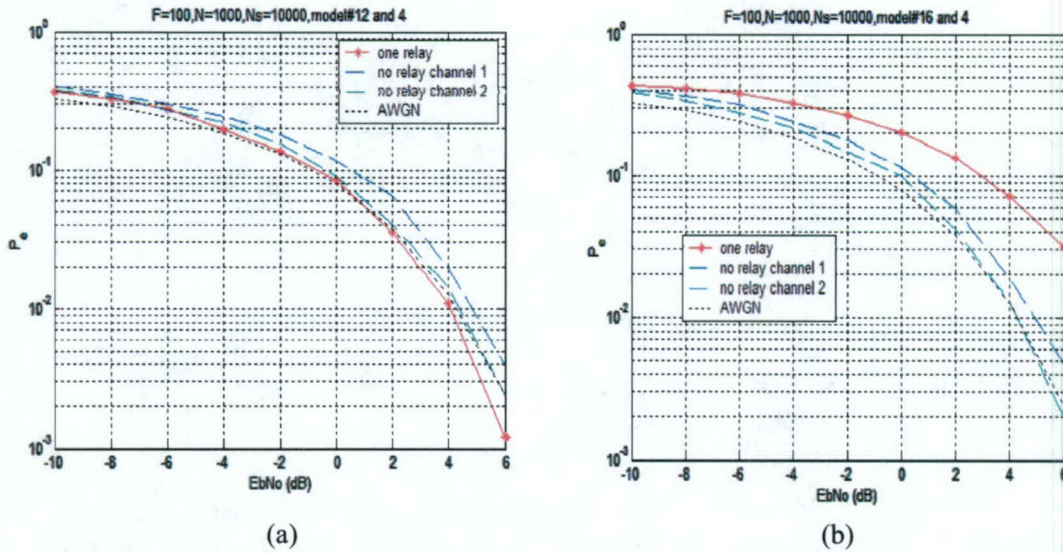
Figure 2.4-3 Performance of cooperative UWB systems. It is assumed that a 100-Finger Rake is used. (a) channel delay profiles 12 and 4 are used; (b): use channel delay profiles 16 and 4 are used.

To provide coherent combining of the signals at the receiver, assume that receiver estimates both channels and feeds back to the other transmitter, respectively. Now, we change the transmit signals to be:

$$S_1 = \sqrt{\frac{E_p}{2}} S * H_2; S_2 = \sqrt{\frac{E_p}{2}} S * H_1;$$ (2.4-6)

where * is the convolution operation. At the receiver:

$$R = S_1 * H_1 + S_2 * H_2 + N = 2\sqrt{\frac{E_p}{2}} S * H_1 * H_2 + N$$ (2.4-7)

As a comparison, Figures 2.4-4a and 2.4-4b plot the performance of the above scheme using the the same UWB channels as Figures 2.4-3a and 2.4-3b. It can be seen that performance benefits are now obtained. However, if N cooperative nodes are used, each transmitter needs the feedback of the other $N-1$ channel estimates which requires significant feedback capacity. The transmitter must then convolve the transmit signal with each channel, which greatly reduces the transmit speed. Due to these shortcomings, we also investigated time reversal techniques to coherently combine signals from different channels.
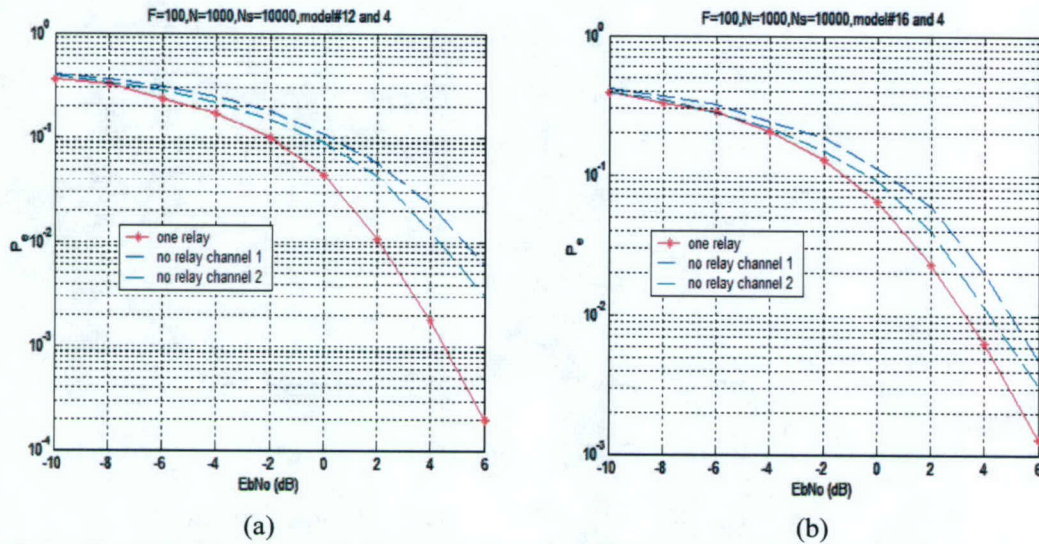
60

Figure 2.4-4 Performance of coherent cooperative UWB systems. 100 Fingers are assumed at the receiver (a) channel delay profiles 12 and 4 are used; (b) use channel delay profiles 16 and 4 are used.

Rewriting the received signal:

$$R = \sqrt{\frac{E_p}{2}} S * h_1^*(-t) * h_1(t) + \sqrt{\frac{E_p}{2}} S * h_2^*(-t) * h_2(t) + N \tag{2.4-8}$$

Figure 2.4-5 shows the received signal at the receiver, due to the autocorrelation function in (2.4-8). The majority of the received energy is located in the peak; therefore, we can simply use a pulse matched filter to detect the signal, instead of Rake receiver, which greatly reduces the complexity of the system. Furthermore, there is no synchronization requirement for the cooperative UWB network, allowing the relay nodes either transmit the relay signal slightly early or late. As long as the signal arrives at the receiver before the next symbol period, the performance of system will not be affected. Also, assuming we have perfect symbol synchronization at the receiver, (2.4-8) becomes:

$$\hat{R} = 2\sqrt{\frac{E_p}{2}} S + \hat{N} \tag{2.4-9}$$

which assumes both channels are normalized. In this way, the received signal power is doubled. Therefore, we expect to see a gain of $10\log_{10} M$ dB, where M is the number of cooperative nodes.

Figure 2.4-6 plots the BER performance of the system with various numbers of cooperative nodes. As the number of nodes increases, the performance gain also increases, although the relative improvement decreases as M increases.
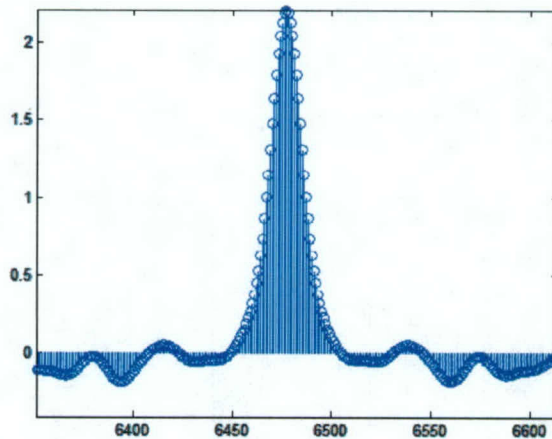
Figure 2.4-5 The received UWB signal before the matched filter.
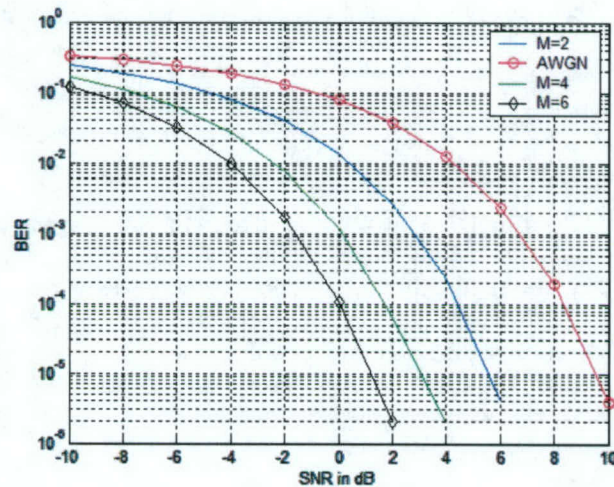

Figure 2.4-6 Performance of coherent cooperative UWB systems using TR method, where *M* represents the number of cooperate nodes.

Although, the TR method shows potential to coherently combine the UWB signals at the receiver with a simple matched filter, it demands that the relay signals arrive at the receiver within a certain time duration. In the next report period, we will focus on waveform adaptation techniques, letting the relay signal adapt its waveform to its partner's transmit signals, instead of merely to the channels.

2.4.3 Importance/Relevance

Software radio technologies are becoming important technologies in the development of military communication systems. The investigation of cross-layer optimization techniques are particularly important for fully exploiting the capabilities of software radio technology. The current work provides the first steps towards understanding a few specific types of cross-layer interaction.

2.4.4 Productivity

Journal publications

1. J. Ibrahim and R.M. Buehrer, " Two-Stage Acquisition for UWB in Dense Multipath," submitted to *IEEE Journal on Selected Areas in Communications*, March 2005.

2. S. Venkatesh and R.M. Buehrer, " A New MAC Protocol for UWB-based Position-Location Networks: Framework and Analysis," submitted to *IEEE Journal on Selected Areas in Communications*, March 2005.

Students supported

Qiao Chen, January. 1, 2005 – present
Swaroop Venkatesh, January. 1, 2005 – present
Jihad Ibrahim, January. 1, 2005 – present

Faculty supported

R. Michael Buehrer, Jan. 1, 2005 – present
Scott Midkiff, Jan 1, 2005 - present

3. TASK 3 Visualization of Wireless Technology and Ad Hoc Networks

3.1 Overview

Task Goal: The goal of this task is to identify and investigate AWINN enabling technologies for the close-in Sea Basing missions.

Organization: The task is directed by Rick Habayeb and Ali Nayfeh. The personnel list follows.

Rick Habayeb, faculty
Ali Nayfeh, faculty
Ehab Abdul Rahman, faculty

Summary: The two main activities during this quarter were: (1) investigating and analyzing the close-in command and control requirements for the Navy Sea Basing missions; (2) identifying AWINN enabling technologies to support Navy Sea Basing requirements.

3.2 Task Activities for the Period

During this quarter we investigated the close-in Command & Control of Sea Basing requirements for sensors and communications. Embedded within the Operational Concept of Sea Basing is the need for effective close-in Command, Control, and Communications (C3) that is secure, available, reliable, scalable, flexible, wireless, and high performance. Our findings revealed that the present close-in Command, Control and Communications could benefit greatly from modernization and technology upgrades. Currently, during the process of rigging for UNREP, telephone lines are passed between ships. One line goes between the two bridges and another telephone line is connected at each transfer station to coordinate the activities at that station. These lines are tended manually. Our analysis determined that the following functions need improvement: (1) high accuracy sensing for soft pickup and landing of cargo, (2) high accuracy sensing and imaging of ships during close-in maneuvers, (3) robust and secure close-in communications and linkages, (4) situational awareness in high sea states, and (5) technology integration.

The enabling technologies that we believe will offer several improvements and new functionalities in the Sea Basing environment are: (1) UWB sensors for close-in ranging and imaging, (2) Software radio with UWB waveform, (3) Mesh topology of Mobile Ad Hoc Network (MMANET), (4) Networking inter and intra distributed sensors, and (5) Visualization environment to integrate high payoff technologies. Our concept to support the close-in sea basing environment is to create a Close-in Digital Environment (CDE). The CDE consists of the following six parts that are also shown in Figure 3-1:

1. Intelligent Networked Sensors (INES)
2. Close-in Situational Awareness (CSA)
3. Close-in Ranging and Position Location (CRPoLo)
4. Cargo Ranging and Landing Sensor (CaRLS)
5. Close-in Wireless Mesh Network (CWMN)
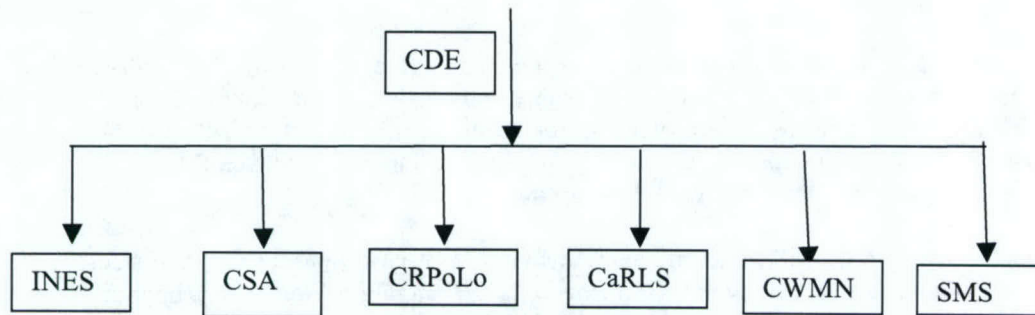6. Ship Motion Sensors (SMS)

Figure 3-1 Close-in Digital Environment (CDE).

The enabling technologies of the INES and CDE will leverage our ongoing research on wireless secure communications, UWB ranging, imaging and communications, Ad Hoc Mobile Network (MANET), Software Defined Radio (SDR), Multi-Input-Multi-Output (MIMO) radio, reconfigurable computers, advanced antennas, real-time middleware, routing and QoS protocols, and the cluster visualization environment CAVE and one-wall CAVE.

There are two integration levels of the INES: Integration of own ship sensors: motion sensors, position and location (PoLo) sensors using range aided integrated GPS/INS, and UWB ranging and imaging sensor. The second INES integration level is the sensors integration of a cluster of ships using a Mesh Architecture of MANET with the capability of sending and receiving data and video streams to enhance the close-in situational awareness of the ships as illustrated in Figure 3-2. The activities of Task 4.3 and Task 2.4 are directly applicable to this Task 3.
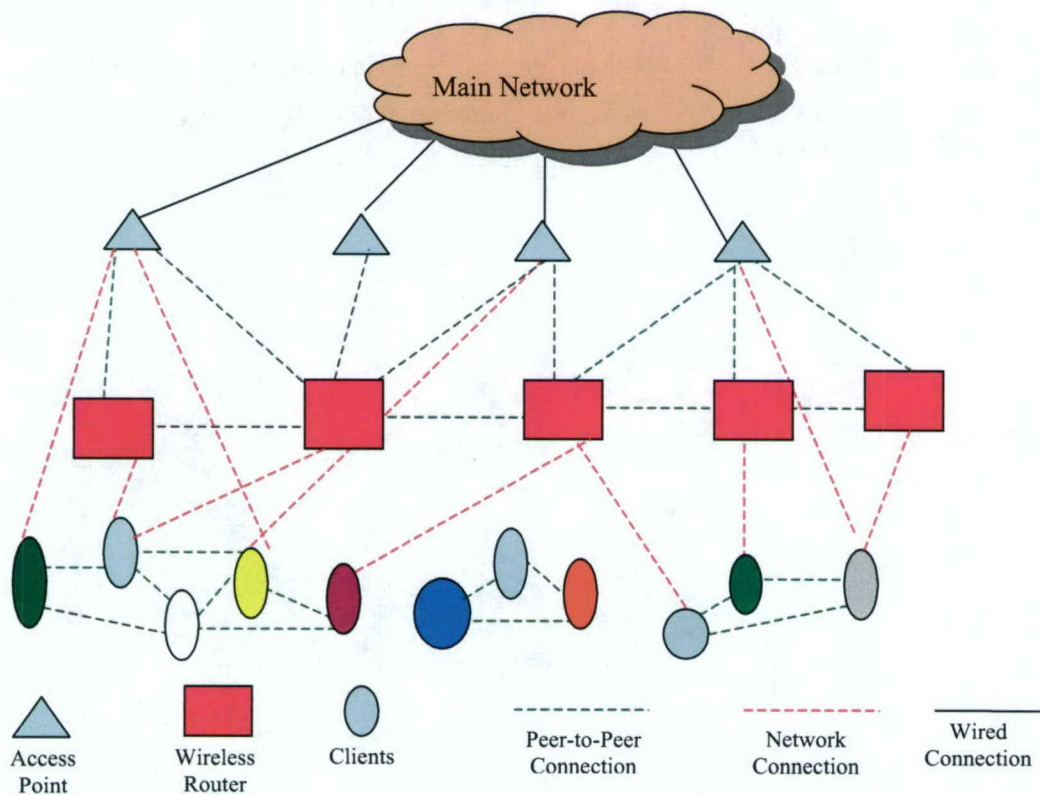

Figure 3-2 Block diagram of a typical mesh network of distributed sensors.

65

Our evaluation of enabling technologies showed that the sensors must be all-weather, jam resistant, of high accuracy, secure, and with minimum multi-path interference. The AWINN UWB task will provide the desired sensor technology. Also, the software radio and the networking tasks will support the close-in communications needs of Sea Basing. Our team has initiated a working relationship with these groups.

Plans for next quarter will focus on integrating the UWB sensor into the laboratory scale model of a crane, and perform accuracy measurements of UWB ranging sensor in the laboratory.

3.3 Importance/Relevance

ForceNet is the Navy implementation plan for Network Centric transformation. There are three fundamental concepts in ForceNet: Sea Shield, Sea Strike, and Sea Basing. Sea Basing is projecting joint operational independence. There are several technological challenges associated with the Navy's vision of Sea Basing. First, a major challenge is the close-in Command, Control, and Communications (C3). Currently, ship-to-ship close-in C3 during UNREP is tedious, time consuming, archaic, and labor intensive. This project will explore, develop, and integrate the high payoff enabling technologies for the close-in sea basing environment.

3.4 Productivity

Related Activities: The group is responding to the Navy RFP for phase II HICASS RFP.

Honors and Recognition
1. A.H. Nayfeh received the Virginia 2005 Lifetime Achievement in Science Award.

2. A.H.Nayfeh received the Lyapunov Award from the ASME for his contribution to the field of Nonlinear Dynamics.

Students Supported
N.Nayfeh – January 25, 2005 to present.
M.Daqaq - January 25, 2005 to present.
O. Marzouk - January 25, 2005 to present.

4. <u>TASK 4</u> Testing and Demonstrations

AWINN emphasizes integration of technologies for ad hoc wireless networks. To facilitate the integration of the several diverse technologies in AWINN, several Technology Integrations Projects (TIP's) have been formulated. Although, any actual demonstration may be weeks or months away, we should be well organized. TIP's form a mechanism to integrate the separate advanced technologies in AWINN. The following sections present our concepts of the TIP's.

4.1 TIP #1: Distributed MIMO UWB sensor networks incorporating software radio

Applications for D-MIMO UWB sensor networks take advantage of UWB's Low Probability of Intercept, its capacity for precision location and ranging, as well as the flexibility offered by SDR architectures to coordinate transmission or reconfigure the radio in real time.

In conjunction with Task 1.2, this task will be exploring range extension as one of the potential benefits of applying D-MIMO to UWB signals. Low-power UWB signals that will be used in a sensor network generally have an extremely limited range—on the order of a few meters. By applying a D-MIMO coordination effort, we believe that it will possible to extend the range of a group of sensors to tens or perhaps even hundreds of meters. Thus, a set of very low power and limited range sensors could be deployed over a local area while still maintaining the ability to transmit signals over large distances.

One potential application is for intrusion detection. A set of UWB sensors could be deployed around an area, and each sensor could monitor, for example, the multipath structure of the channel between adjacent nodes. Changes in the multipath structure would likely be caused by a person or object moving into the area. Additionally, the UWB sensors could use a passive position location technique to track the person or object motion. The sensors could then use a D-MIMO coordination to transmit the intrusion detection and its location back to a control center.

UWB sensors could also be used to aid GPS positioning information on a set of UAVs. The precision positioning information provided by the UWB sensors could be used to fine tune the GPS location information and allow the UAVs to fly in a very tight formation, possibly close enough to appear as a single target on a RADAR. The D-MIMO topology could be used to relay position information back to a control center or other UAV squadrons. The software radio architecture allows the UWB receivers to function as both sensor nodes as well as UWB communication systems, or even more traditional broadband communication systems.

4.2 TIP #2: Close-in UWB wireless with applications to Sea-Basing

4.2.1 Overview

Task Goal: The goal of this task is to demonstrate the usefulness of UWB in close-in communications and ship-to-ship cargo transfer for sea-basing operations.

Organization: This task is managed by Dr. R. Michael Buehrer

Dr. R. Michael Buehrer, faculty
Swaroop Venkatesh, GRA
Haris Volos, GRA

Summary: In this quarter we designed a set of experiments that will demonstrate the usefulness of UWB systems for ship-to-ship cargo transfer.

4.2.2 Task Activities for the Period

Subtask 4.2.2a UWB-based Ranging for Ship-to-Ship Cargo Transfer

Impulse-based Ultra-Wideband (UWB) pulses provide extremely accurate (sub-nanosecond) time-resolution. This accurate time-resolution translates to accurate spatial resolution in UWB radar applications. Based on the time-of-arrival (TOA) of UWB pulses, ranges can be measured accurately to the order of inches. Additionally, this accuracy can be maintained in the presence of severe multipath propagation due to the resistance of UWB to multipath fading. We, thus, propose the use of UWB pulses in the Sea Basing operation as described below.

The Sea Basing scenario, shown in Figure 4.2-1 includes a crane located on a ship ("source") attempting to unload a crate to a second ship ("destination") as smoothly as possible, even under turbulent weather conditions. Due to the motion of the source and the destination, large scale variations in the relative heights and orientations of the ships are possible. In order to ensure secure transfer of the cargo, the source could compensate for its own motion using a control system employed within the crane. However, this control system also needs to take into account the motion of the destination.
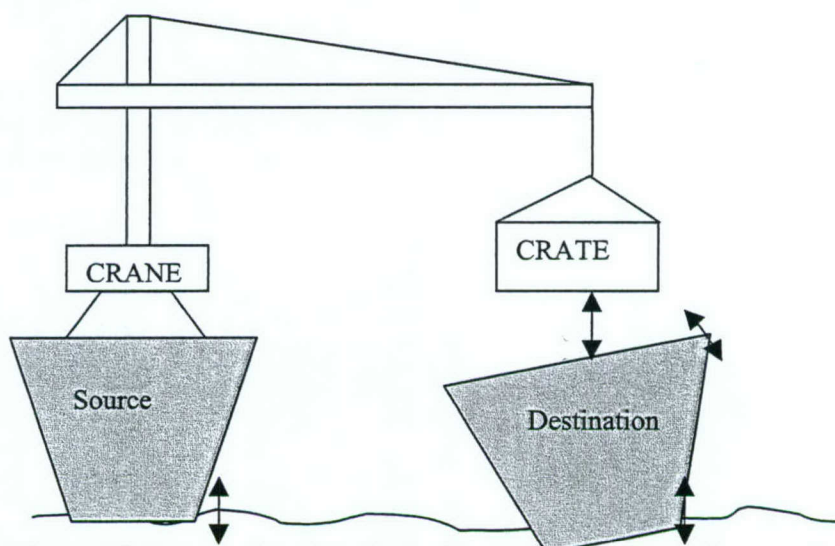

Figure 4.2-1 Illustration of the basic ship-to-ship cargo transfer operation.

In order to measure the destination's motion and orientation, and to supply these values to the crane's control system, we propose the use of UWB TOA-basing ranging techniques. Consider the simple setup of a UWB transmitter and receiver shown in Figure 4.2-2. The transmitter and receiver are separated by a distance d_0, and are suspended a height h above the floor.
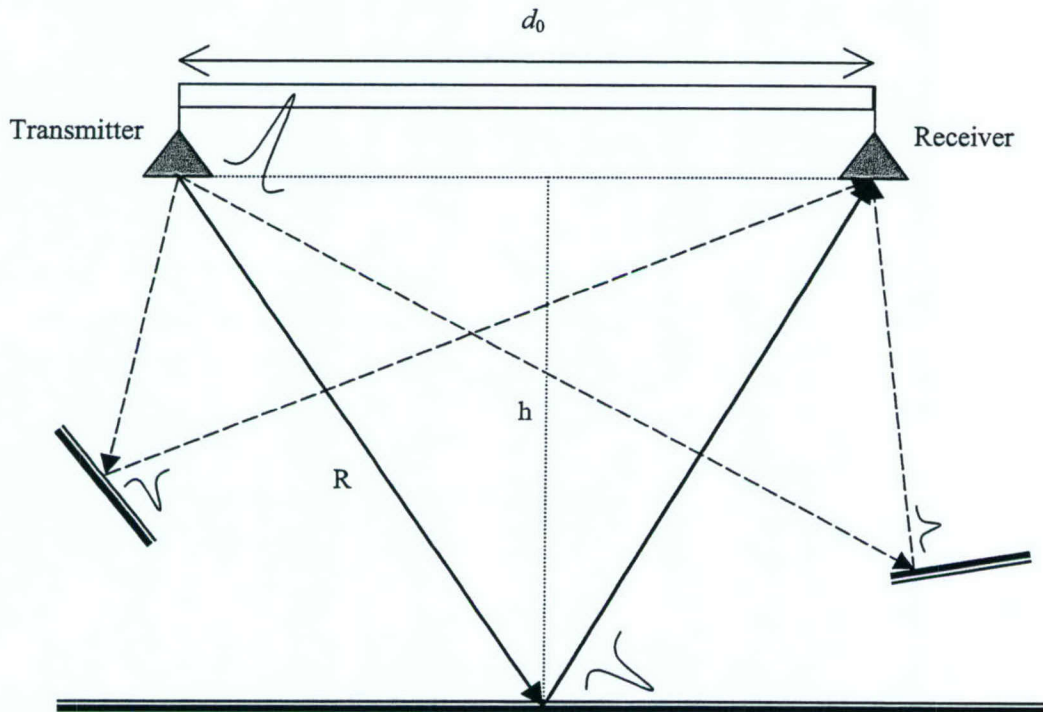

Figure 4.2-2 Simple setup of a UWB transmitter and receiver suspended above the ground.

The waveform measured at the receiver includes reflections of the transmitted pulse from scatterers in the environment or *multipath*, as seen in Figure 4.2-3. As the floor is, with high probability, the scatterer with the largest radar cross-section, we expect that the pulse reflected by the floor will be the strongest multipath component in the received profile, provided there is no Line-of-Sight (LOS) path between the transmitter and the receiver (this can be effectively guaranteed through proper shielding). The distance traveled by a pulse from the transmitter to the receiver after reflection by the floor can be estimated accurately based on the TOA of this reflected pulse. Using this distance ($2R$) and the distance between the transmitter and the receiver (d_0), the height of the setup above the floor can be estimated using Pythagoras' theorem:

$$\hat{h} = \sqrt{R^2 - \frac{d_0^2}{4}}$$

The destination's deck can also have an orientation different from that of the source, and in order to measure this orientation, our proposed design consists of four UWB ranging devices placed at the four corners of the crate transfer system (perhaps attached to the crane claw) that determine the distance from each side of the crate to the ship's deck. This design is illustrated at Figure 4.2-4.
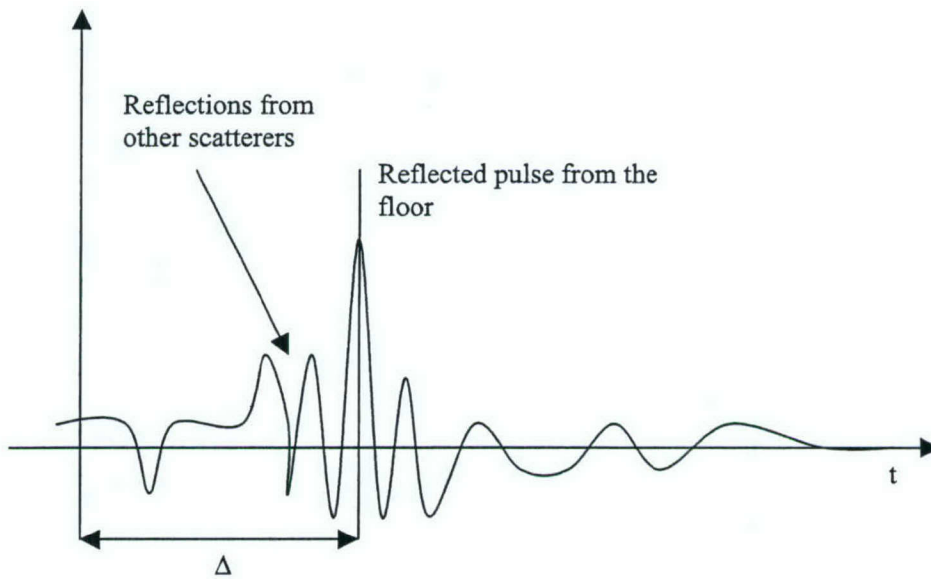
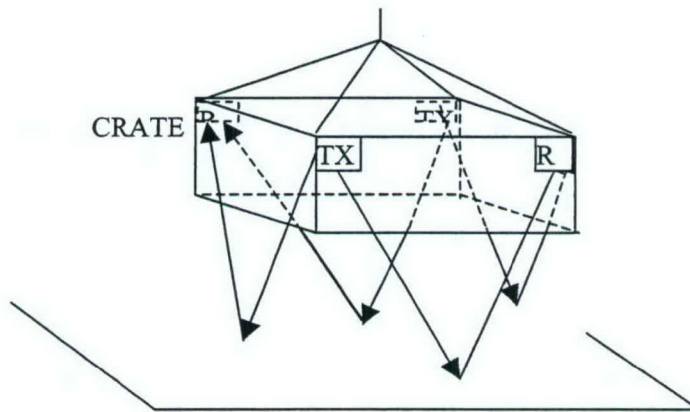**Figure 4.2-3** The multipath profile seen at the receiver.

Figure 4.2-4 Ranging sensor locations.

Based on this design, each pair of sensors can measure the height above the deck from the midpoint between them, and therefore can also determine the orientation of the deck relative to the plane of the sensors. In order to demonstrate this, consider a pair of sensors, with the deck oriented at an angle φ as shown in Figure 4.2-5. We assume that the sensors are able to estimate the distance $R = a_1 + a_2 + b$ based on the multipath profile. Using some basic trigonometric identities, we have the following relations:
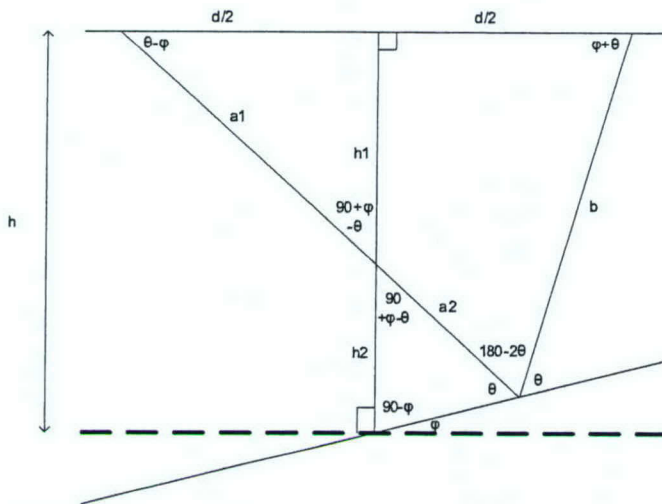
Figure 4.2-5 Angles and distances when the destination's deck has a different orientation from the crate.

$$R = a_1 + a_2 + b = \frac{d\cos\varphi}{\cos\theta} \Rightarrow \theta = \arccos\left(\frac{d}{R}\cos\varphi\right)$$

$$h = h_1 + h_2 = h_1 + \frac{a_2\sin(\theta)}{\cos(\varphi)} = \frac{d}{2}\tan(\theta - \varphi) + \frac{d\sin(\theta)}{\cos(\varphi)}\left[\frac{\sin(\theta + \varphi)}{\sin(2\theta)} - \frac{1}{2\cos(\theta - \varphi)}\right]$$

The given parameters are R and d and the unknowns are h, φ and θ. Based on the above equations, we can solve for two of the unknowns with the third as a parameter. Based on the data from the four transmit-receive pairs, we can iterate to find the solution in terms of the heights of the midpoints of the sides of the crate above the ship's deck.

Further Work: In the coming quarter, we will be looking at the following aspects of the problem:

1. An iterative scheme to solve for the height and orientation of the crate relative to the destination's deck.

2. The accuracy of the TOA-based ranging in severe multipath

3. The effect of the accuracy of ranging and other parameters on performance

4. A link budget for the system

5. Simulation of system performance

4.2.3 Importance/Relevance

Sea Basing is a critical application for the Navy. Close-in communications and ship-to-ship cargo transfer remain important technological challenges that need to be addressed. The work in this task has the potential to be tremendously useful for the Navy.

71

4.2.4 Productivity

<u>Students supported</u>
Swaroop Venkatesh, January. 1, 2005 – present

<u>Faculty supported</u>
R. Michael Buehrer, Jan. 1, 2005 – present

4.3 TIP #3: Secure Ad Hoc Networks

4.3.1 Project Description

The testing and demonstration of secure ad hoc networks will involve integration and testing along two related tracks. In the first track, activities within Task 2.1 (Ad Hoc Networks) will be integrated, tested, and demonstrated. Capabilities including policy-based quality of service (QoS), security based on distributed certificate authorities (DCAs) for key management and trust grading, and mobile ad hoc network (MANET) routing support QoS and security functionality and as a means to demonstrate cross-layer design. Cross-layer design techniques from Task 2.4 will be reviewed and incorporated as appropriate.

In the second track, we will integrate real-time middleware from Task 2.2 with the integration of QoS, security, and routing as discussed above and as investigated in Task 2.4. Specifically, we will investigate and develop methods and mechanisms to integrate policy-based quality of service (QoS) capabilities at the network level, and perhaps at the link layer, with real-time services offered by middleware.

4.3.2 Demonstration Description

Table 4.3-1 lists the demonstration components that are currently planned for two scenarios. Scenario 1 relates directly to Task 2.3 and involves the integration of network services with an application based on the time-utility function real-time middleware. Scenario 2 involves network support for a video sensor application provided by Tom Hou. We will adjust plans based on results from related tasks.

Table 4.3-1 Demonstration Components for the Two Scenarios

Scenario 1: Real-Time Application	Scenario 2: Video Sensor Network
Real-time middleware	Distributed video coding application
Security and key management system	Security and key management system
Policy-based quality of service	Policy-based quality of service
OSPF-MCDS-MC and/or OLSR-MC routing	OSPF-MCDS-MC and/or OLSR-MC routing
TopoView network monitoring	TopoView network monitoring
Performance monitoring tools	Performance monitoring tools
Topology emulation	Topology emulation

The components of the different scenarios listed in Table 4.3-1 are currently envisioned to be the same except for the application (or application plus middleware in the case of Scenario 1) being supported. The security, QoS, and routing components are discussed further in Section 2.1 of this report. Note that OSPF-MCDS-MC is a multi-channel version of the Open Shortest Path First with Minimum Connected Dominating Sets (OSPF-MCDS) MANET routing protocol. OLSR-MC is a multi-channel version of the Optimized Link State Routing (OLSR) MANET routing protocol. The topology view (TopoView) and topology emulation tools are carried over from the previous NAVCIITI project. It is envisioned that additional performance monitoring and configuration control tools will be developed as part of Subtask 2.1(e) and used in the demonstrations.

4.3.3 Cooperative AWINN Elements

Test and demonstration requires the inputs from AWINN tasks as specified in Table 4.3-2.

Table 4.3-2 Inputs from Cooperative AWINN Elements

Task (Subtask)	Inputs
2.1a	Prototype implementation of a policy-based QoS scheme
2.1b	Prototype implementation of MANET security and key management scheme
2.1c	Optimized prototype implementation of a MANET routing, specifically OSPF-MCDS-MC and/or OLSR-MC
2.1e	Performance monitoring tools; enhanced TopoView; enhanced topology emulation
2.1 (Hou)	Video sensor application and test bed components
2.2	Real-time middleware
2.4	Cross-layer optimization elements that can be integrated into the test bed for testing and demonstration purposes.

4.3.4 Cooperative Non-AWINN Elements

At this time, no non-AWINN components are required (except for tools and equipment carried over from the NAVCIITI project).

4.3.5 Schedule of Activities

A general schedule is provided in Table 4.3-3.

Table 4.3-3 Schedule of Activities

Activity	Date
Plan test infrastructure	July-September 2005
Acquire test bed hardware and software, as needed	September-November 2005
Deploy test infrastructure	October-November 2005
Integration of real-time middleware and application	November-December 2005
Testing and demonstration of real-time middleware and application	January-February 2006
Integration of video sensor network application	March-April 2006
Testing and demonstration of video sensor network application	May-June 2006

4.4 *TIP #4:* Integration of Close-in UWB wireless with ESM crane for Sea Basing applications

4.4.1 Overview

Task Goal: The goal of this task is to demonstrate the usefulness of UWB in close-in communications and ship-to-ship cargo transfer for sea-basing operations.

Organization: This task is managed by Dr. A. H. Nayfeh
   Dr. A. H. Nayfeh, Faculty
   Dr. E. Abdel-Rahman, Post Doc
   N.A. Nayfeh, GRA

Summary: We have identified a set of experiments that will demonstrate the usefulness of UWB systems for ship-to-ship cargo transfer:

- Measure an up and down moving object on a shaker. For this purpose, we identified two shakers in the Nonlinear Dynamics Laboratory: a shaker with a small stroke and another with a large stroke.
- Measure the orientation of a plate placed on top of a shaker whose head moves up and down.
- Measure the position of a point and the orientation of a plate on top of a shaker head that moves horizontally.
- Measure the position of a point and the orientation of a plate mounted on top of the Stuart platform in the Crane Control Laboratory; see Figure 4.4-1.. This platform has six degrees of freedom: heaving, pitching, rolling, surging, yawing, and swaying.
- Integrate the UWB with the Crane Control System and demonstrate the performance of the total system experimentally.

4.4.2 Further Work

In the coming quarter, we will coordinate with Dr. Buehrer to conduct the above identified experiments that culminate in demonstrating cargo transfer between two moving platforms.

4.4.3 Importance/Relevance

The proposed work has the potential of being very useful to the Navy's Transformational Sea-Basing System. The success of Sea Basing depends on the ability to sustain logistic operations with significantly reduced reliance on land bases. This requires the development of a high capacity, high reliability at-sea capability to transfer fuel, cargo, vehicle, and personnel in rough seas while underway from commercial container ships to large sea basing ships and then to smaller ships. The wave-induced motion of the crane ship can produce large pendulations of the cargo being hoisted and cause the operations to be suspended

4.4.4 Productivity

Students supported
   N. Nayfeh, January. 1, 2005 – present
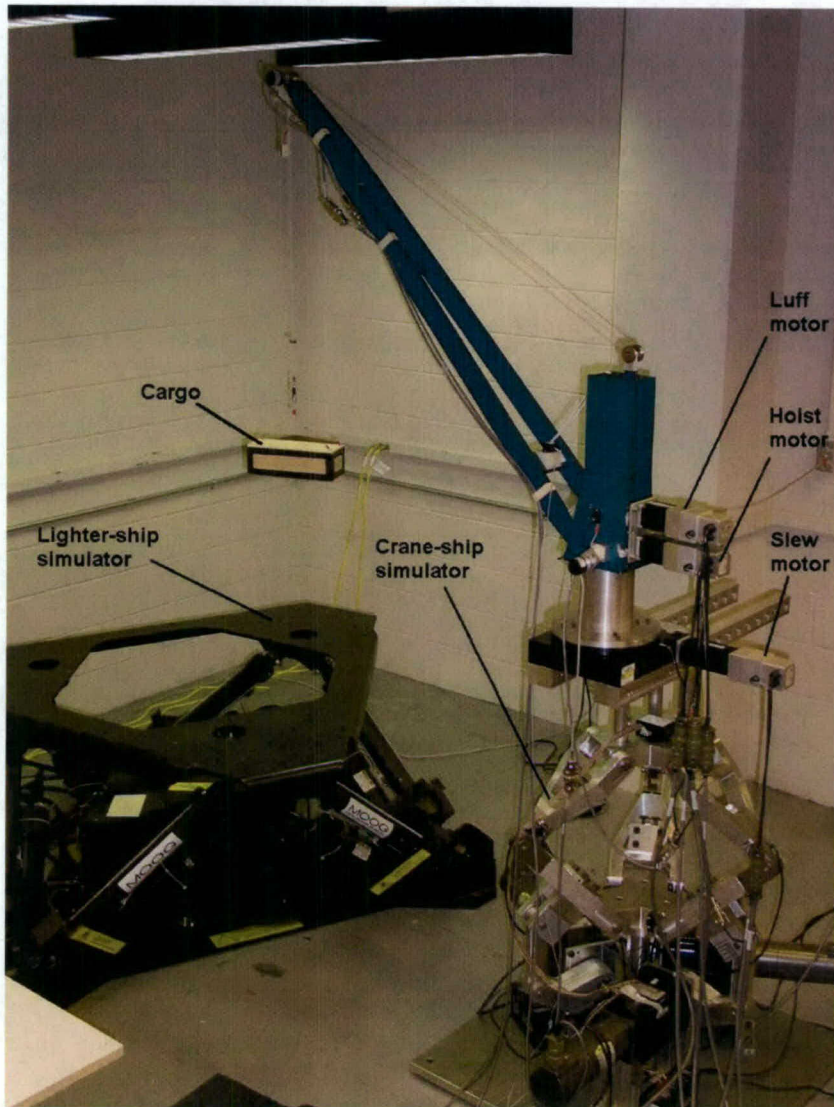
Figure 4.4-1 Experimental setup for demonstrating the full Crane Control System.

5. FINANCIAL REPORT

Total Project Budget/Actual
(Equipment, Personnel and Other Direct Costs)
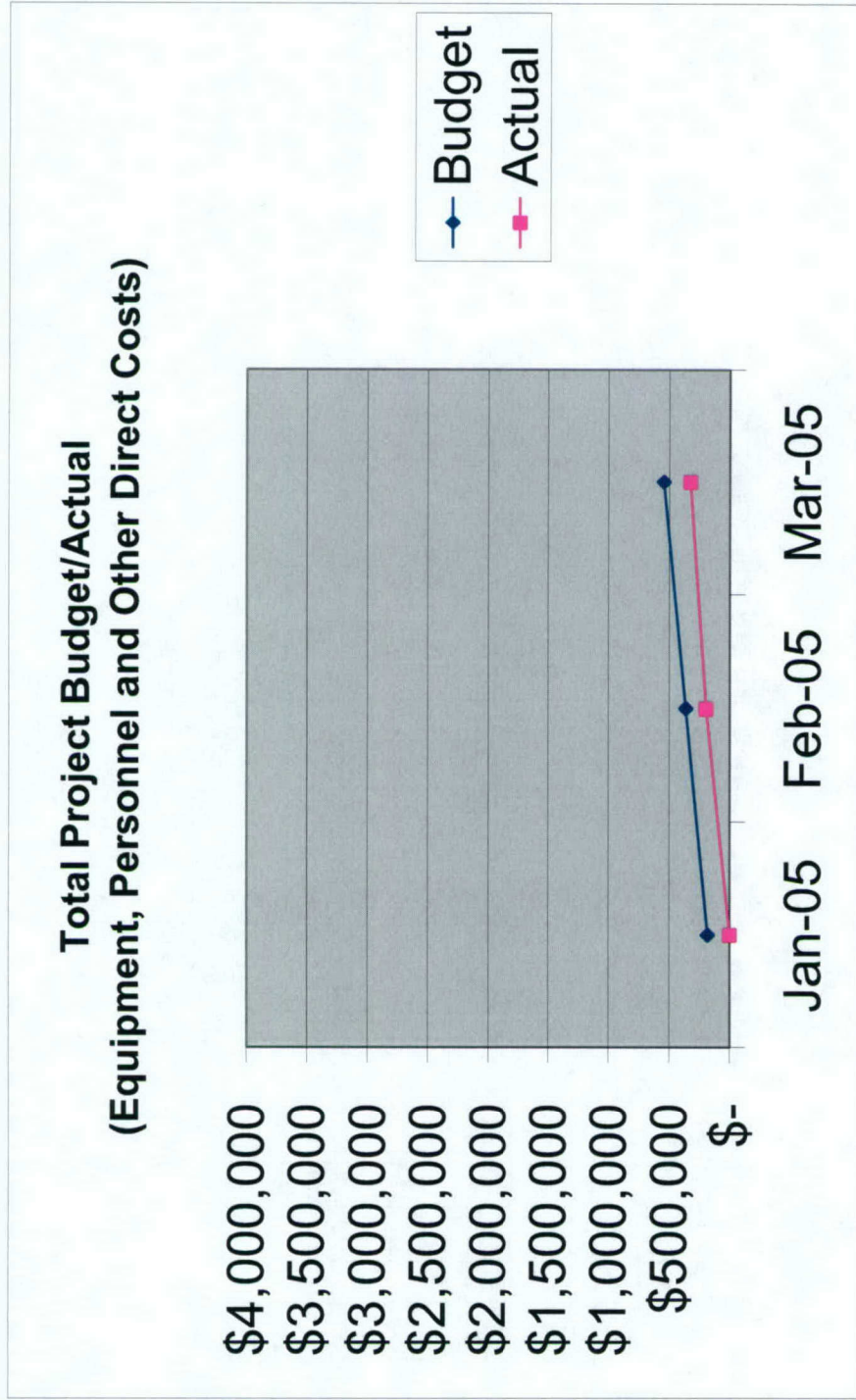
NOTE: The University reporting period begins on the 25th and runs through the 24th of the following month. For example, charges in March are for Feb. 25 – Mar. 24. Accounts were initialized on Jan. 27, 2005; thus most of January's charges appear in the February Report.